LUND UNIVERSITY

LTH

FACULTY OF ENGINEERING

Faculty of Engineering LTH
Department of Biomedical Engineering

Master's Thesis in Biomedical Engineering

January 2023 - June 2023

Association of a Wristband PPG and an ECG Sensor - Analysis, Synchronization and Robustness

---

Author: Mattéo Hochart

Supervisor:
Frida Sandberg

Examiner:
Martin Stridh

Abstract

Context: The CardioHolter, developed by Kaunas Institute of Technology, Lithuania, has been used in previous studies on cardiovascular behavior at the Department of Biomedical Engineering at Lund University. This equipment associates two finger photoplethysmography (PPG) sensors and an electrocardiogram (ECG) sensor. It is robust and efficient but very bulky.
The CardioHolter equipment is getting outdated and hence, new equipment is needed for future chamber exposure studies.
The equipment should be easy to use for the study nurse and comfortable for the study participants and the acquired data should be of sufficient quality. This is why another solution is explored with this thesis.

Objective: The objective of this project is to investigate the feasibility of replacing the CardioHolter by the association of a Wristband PPG sensor (Empatica Embrace Plus Wristband PPG) and an ECG sensor (Bittium Faros 360 ECG) in a future chamber exposure study.

Methodology: The first phase of the project is the data acquisition with the CardioHolter, the Empatica Embrace Plus and the Bittium Faros 360. Then the characteristics of the signals gathered are analyzed and compared in order to know the quality and robustness of each signal.

Conclusion: The signals of the Faros and Empatica devices are robust and of good quality, but one problem remains: the synchronization between both devices.

Acknowledgements

I would firstly like to thank my supervisor at LTH Frida Sandberg for her guidance, advice and precious help. Thanks to Frida I have kept a consistent rhythm of work during the whole thesis, and I have been sure I was always sure not to lose myself in a field I discovered during the thesis. I also thank Lund University and more particularly LTH for welcoming me this year and my home school, Centrale Nantes, for giving me the opportunity to complete this year in Lund.

Abbreviations

BP: *Blood pressure*
ECG: *Electrocardiogram*
HF: *High frequency power*
HR: *Heart rate*
HRV: *Heart rate variability*
LF: *Low frequency power*
MAE: *Mean absolute error*
PPG: *Photoplethysmogram*
PTT: *Pulse transit time*
RMS: *Root mean square*
RMSSD: *Root mean square of successive RR-intervals differences*
SDRR: *Standard deviation of the RR-interval*

Contents

1 Introduction

1.1 Aim

Biomedical engineering is one of the fastest growing fields of technology [1]. Taking its roots in the 1780s, this field has never stopped its development through the centuries, going from what was called “animal electricity” to modern biomedical engineering using state of the art technologies. Biomedical engineering has undergone a meteoric evolution in the second half of the XXth century with the apparition of computers leading to the development of high technology devices.

“Wearable devices are becoming widespread in a wide range of applications, from healthcare to biomedical monitoring systems, which enable continuous measurement of critical biomarkers for medical diagnostics, physiological health monitoring and evaluation” [2]. Wearable devices used in biomedical engineering have a certain number of characteristics, making them useful and pertinent depending on the application. Of course, every device has its proper purpose depending on what it measures such as temperature, heart pulses, blood pressure, glucose level, physical activities or even insulin levels [3]. But for different devices measuring the same physiological indicators, it is pertinent to compare not only their quality (precision, accuracy, robustness) but characteristics that are less technical like their bulkiness, their weight, their user interface, their price or their use complexity to compare their use convenience.

This thesis will focus on 3 devices particularly. Indeed, the Biomedical Engineering department in Lund University has led studies exploiting electrocardiography and photoplethysmography using a device called the CardioHolter. However, even though this device has a high signal quality [4], it begins to be outdated because of its bulkiness, the number of wires used and the need of a computer in proximity. This is why this thesis will explore the possibility of replacing it by the association of the electrocardiogram Bittium eMotion Faros 360 [5] and the photoplethysmogram Empatica Embrace + [6].

This paper will discuss the general principles of PPG and ECG signals, including the different ways to acquire them and their characteristics to answer the question: “Can the CardioHolter equipment be replaced by the Empatica wristband and Faros 360?”. From these signals, heart rate, heart rate variability, pulse transit time and pulse decomposition will be computed and analyzed to compare results from the three different devices. The possibility of assessing PTT using Empatica Embrace + and Faros 360 will be explored. Finally, the following question will be studied: “Are PPG pulse morphology changes in CardioHolter finger PPG also visible in Empatica wristband PPG?”.

The results will be presented and discussed to conclude on the possibility of replacing the CardioHolter with the combination of the Faros 360 and the Empatica Embrace + device.

2 Background

2.1 General Principles

2.1.1 PPG Signals

Photoplethysmography (PPG) is a non-invasive technique that measures blood volume changes in the microvascular bed using a light source and a detector. The PPG signal is widely used in clinical settings for pulse rate and oxygenation function and in research for various applications.

A PPG pulse (Figure 2.1) is formed by the interaction of the left ventricle and the vessels [7] and is decomposed in two parts. The first part is characterized by a high slope until a maximum value called the systolic peak, corresponding to the contraction of the heart muscle. After that peak there is a decreasing slope until the dicrotic notch before an inflection point for an increasement until the second peak called the diastolic peak, corresponding to “the reflected wave through the blood transmitted to the lower extremities and sent back to the aorta” [7]. It then gets its initial position back.

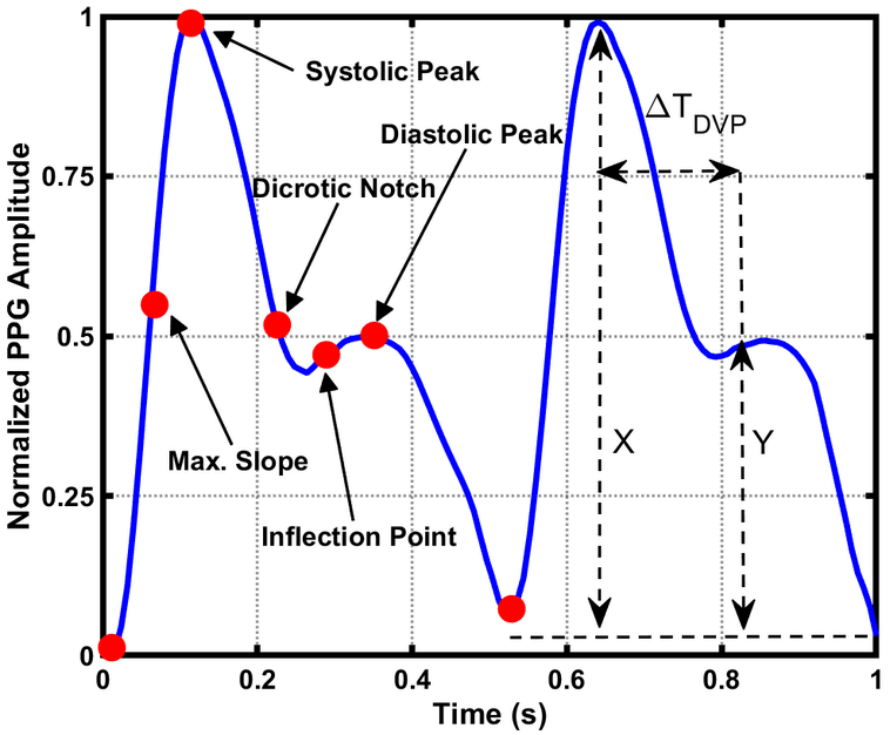

Figure 2.1: PPG pulse waveform [8].

There are two primary methods for acquiring PPG signals: reflection and transmission. In reflection mode, the light source and detector are placed on the same side of the tissue. In this method, the PPG signal is generated by the reflection of the light by the tissue. In transmission mode, the light source and detector are placed on opposite sides of the tissue and the PPG signal is generated by the absorption and the transmission of the light through the tissue.

The PPG signal consists of several components, including the Alternating Current (AC) component and the Direct Current (DC) component. The DC component is due to the non-pulsatile changes in blood volume and tissue absorption whereas the AC component is due to the pulsatile changes in blood volume. So, it is the AC component of the PPG signal that is typically used for analysis because it is correlated with changes in blood flow and oxygen saturation.
The PPG signal can be affected by various factors such as motion artifact, ambient light, and skin pigmentation. Motion artifact occurs when the tissue moves relative to the light source and detector, resulting in changes in the signal amplitude and shape. Ambient light can interfere with the PPG signal by introducing noise or saturating the detector. Skin pigmentation can affect the amount of light that is absorbed by the tissue, which can impact the signal amplitude.

There are several advantages of using PPG over other physiological measurements such as electrocardiogram (ECG). PPG measurements are non-invasive as they are obtained easily without requiring electrodes (required for ECG acquisition) or other invasive instruments. PPG signals can also provide information about the peripheral circulation, which is not directly measured by the ECG.

PPG signals can be obtained from various parts of the body, such as the finger, earlobe, toe, forehead, and wrist. Finger PPG signals are commonly used in clinical settings for monitoring cardiovascular function. However, wrist PPG signals have become increasingly popular in recent years due to their convenience and versatility. Wrist

PPG signals can be obtained using wearable devices such as smartwatches and fitness trackers, which allow for continuous monitoring in daily life.

Compared to traditional methods of blood pressure measurement, wristband-based PPG sensors are non-invasive, small and portable, and can provide continuous monitoring. These advantages can make blood pressure monitoring more convenient and less intimidating for patients, improve patient compliance, and reduce measurement errors. Even though PPG based BP is still experimental, continuous monitoring can be particularly valuable for patients who have fluctuating blood pressure or who need to track their blood pressure throughout the day [9].

Compared to finger PPG sensors, wristband PPG sensors are more comfortable to wear for extended periods of time as they do not restrict hand movements or cause discomfort to the fingertips. Wristband PPG sensors are also less sensitive to motion artifacts and skin color changes compared to finger PPG sensors so they can provide more stable signals. In addition, wristband PPG sensors can be used for continuous monitoring of the heart, which can be useful for detecting changes in cardiovascular health over time.

However, there are also some cons to using wristband PPG sensors. Indeed, they may not be as accurate as finger PPG sensors for measuring heart rate and heart rate variability, particularly during intense physical activity or in patients with arrhythmias. Moreover, wristband PPG sensors may be more susceptible to environmental factors, such as changes in temperature or humidity, which can affect the quality of the signal [10].

Transmitted PPG signals are acquired by placing a light source and a detector on opposite sides of a body part, such as a finger. The light source emits light, and the detector measures the amount of light that passes through the tissue to reach it. The resulting signal is a waveform reflecting the changes in blood volume in the tissue because the amount of light passing through the tissue varies depending on the blood flow.

Reflected PPG signals, on the other hand, are acquired by placing both the light source and the detector on the same side of the body part. The light source emits light, and the detector measures the amount of light that is reflected back from the tissue. As for transmitted signals, the resulting signal is a waveform reflecting the changes in blood volume in the tissue as the amount of reflected light varies depending on the blood flows.

In terms of waveform morphology, transmitted and reflected PPG signals can look quite different. For two PPG signals acquired at the same position (here the index finger), transmitted PPG signals (Figure 2.2) typically have a larger amplitude and a more well-defined waveform than reflected PPG signals due to a higher variation in light transmitted than in light reflected. Reflected PPG signals (Figure 2.3) have a smaller amplitude and a more variable waveform, since the amount of light that is reflected from the tissue can be affected by factors such as skin pigmentation and tissue thickness.

The transmitted waveform is characterized by an initial sharp peak followed by a dicrotic notch and a small secondary peak. The waveform then descends gradually before returning to the baseline.

Furthermore, the height of the initial peak reflects the amplitude of the arterial pulse pressure, while the height of the secondary peak represents the amplitude of the reflected wave. The dicrotic notch corresponds to the closure of the aortic valve, and its depth reflects the level of peripheral vascular resistance [11].

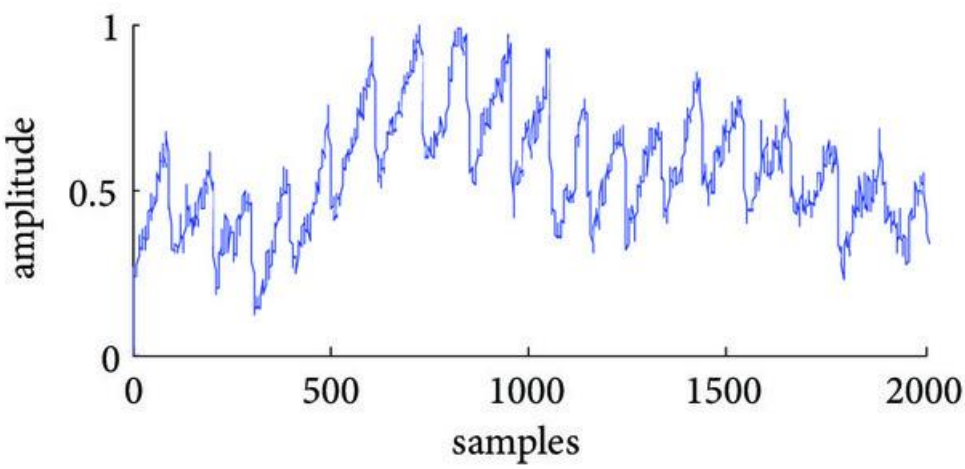

Figure 2.2: Transmitted PPG signal.

The reflected PPG signal has the same general shape with several differences depending on the device used. It is usually less noisy than the transmitted PPG signal [12].

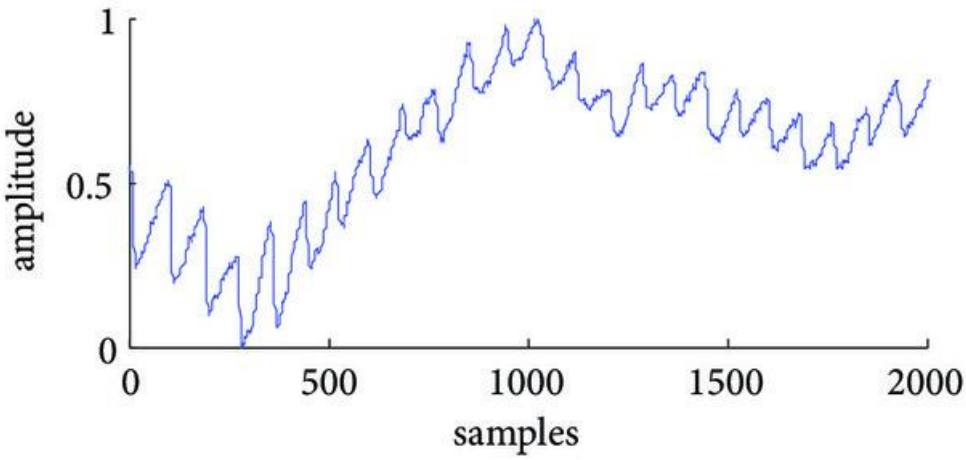

Figure 2.3: Reflected PPG signal [13].

2.1.2 ECG Signals

Electrocardiography (ECG) is also a technique used to measure the electrical activity of the heart. These signals have clinical uses for the diagnosis and monitoring of various heart conditions.

ECG signals are obtained by placing electrodes on the skin, typically on the chest. The electrodes are connected to an ECG machine amplifying and recording the electrical signals produced by the heart. ECG signals are usually recorded for a few seconds to a few minutes, and the resulting waveform is displayed on a screen or printed on paper.

The key characteristic of ECG signals is their waveform: the graphical representation of the heart electrical activity over time. Indeed, the ECG wave shapes consist of a series of peaks and valleys including the P wave, QRS complex and T wave (Figure 2.4).

The P wave represents the electrical activity due to the atria's contraction to push blood into the ventricles. The QRS complex represents the electrical activity due to the ventricles' contraction to pump blood out of the heart. The T wave represents the repolarization of the ventricles, as they prepare for the next cardiac cycle. The components providing important and interesting information about the heart behavior are the duration, amplitude and morphology of these waves [14].

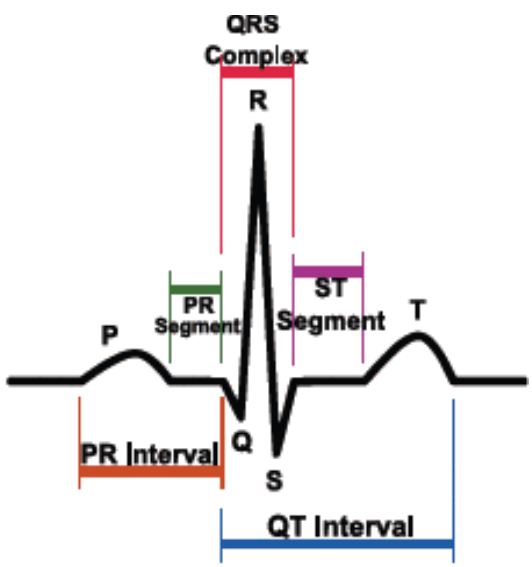

Figure 2.4: ECG pulse waveform.

2.2 Heart Rate and Heart Rate Variability

The heart rate (HR) is the measurement of the number of pulses per minute. It can be measured for every beat by measuring the lag between two pulses and then converted as a value in pulses per minute. For this study, it will be necessary to detect each pulse's peak for the HR measurement.

Heart Rate Variability (HRV) is the measurement of the variations of cardiac rhythm as the human heart rate is not constant with time, depending on many factors (physical activities, emotions, body temperature, stress, hydration or medicines can affect the HR). So, by knowing the HR over a certain lapse of time we can deduce the HRV which has a key influence in determining prognosis post myocardial infarction and the risk of sudden cardiac death [15]. HRV metrics are known with the HRV computation to detect possible abnormalities [16]. Among those are the standard deviation of RR intervals (SDRR), the root mean square of successive RR interval differences (RMSSD), the power of the low-frequency band (LF) and the power of the high-frequency band (HF) and the ratios LF/HF and SDRR/RMSSD [17].

2.3 Pulse Transit Time

“Pulse transit time (PTT) has been originally used, at rest, in clinical settings (psychophysiological, arousal studies) as a measurement of blood pressure. In most of the studies this parameter was suggested to assess arterial stiffness and more recently as a blood pressure surrogate. Most importantly, pulse transit time has been used as a measure of vascular health and condition across life span in different populations” [18].

PTT is the time (Figure 2.5) needed from the cardiac pulse wave to travel from the heart to the wrist or the finger (depending on the PPG device). “In practice, it is measured as the difference between the position of the peak of the R-waves on the ECG and the onset of the corresponding pulse on the PPG signal” [19]. As for the HR measurement, it is necessary to detect every pulse’s peak.

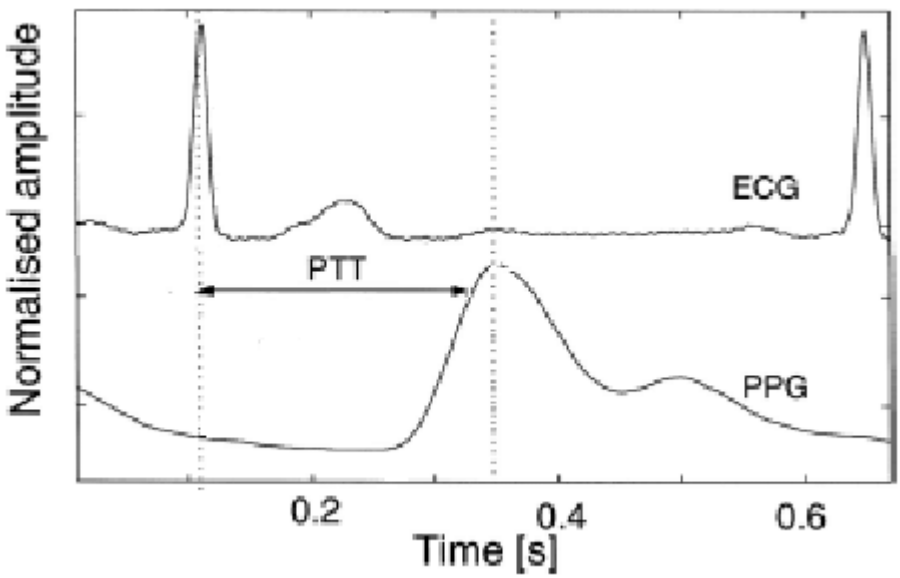

Figure 2.5: PTT definition [20].

The order of magnitude of PTT is approximately 0.2 s [21]. This implies the need for a perfect synchronization between the ECG and PPG clocks to have a decent measurement of the PTT.

2.4 Pulse Decomposition

The PPG pulse decomposition in Gaussian functions is an accurate manner for the PPG pulse waveform analysis. Moreover, this method is also efficient even for weak or noisy signals, or when the diastolic part of the pulse is not damped out [22].

Yves Meyer has demonstrated that every curve can be decomposed as a sum of Gaussian functions [23]. The modelling of PPG pulse waveforms by curve fitting with Gaussian functions “constitutes a simple and accurate manner for reproducing and analyzing waveforms” [19].

There are several ways of decomposing a PPG pulse in Gaussian functions. Two methods are studied here (Figure 2.6): the first one is the decomposition of each peak in the sum of two distinct Gaussian functions and the second the decomposition of the entire pulse in the sum up to three Gaussian functions [19].

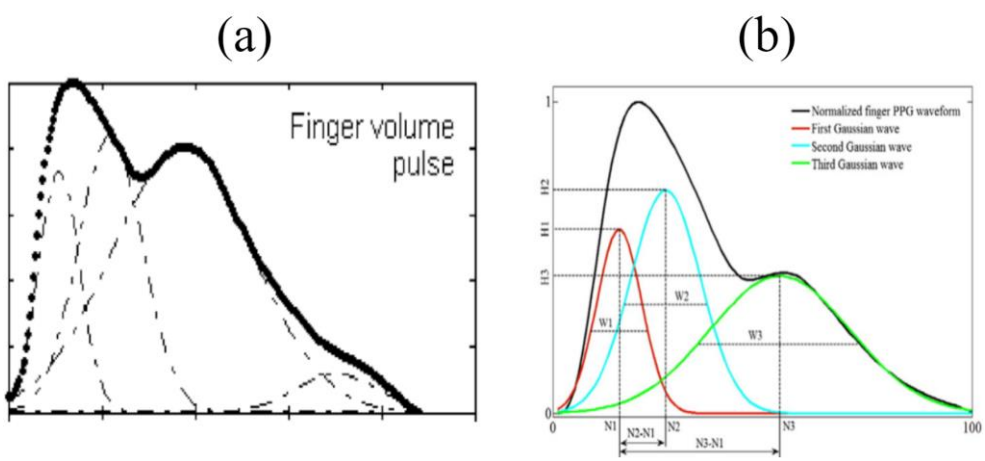

Figure 2.6: Pulse waveform decomposition using Gaussian curve fitting [19].
(a) Decomposition of each peak in 2 Gaussian curves
(b) Decomposition of the entire pulse in 3 Gaussian curves

3 Methods

3.1 Devices

3.1.1 CardioHolter

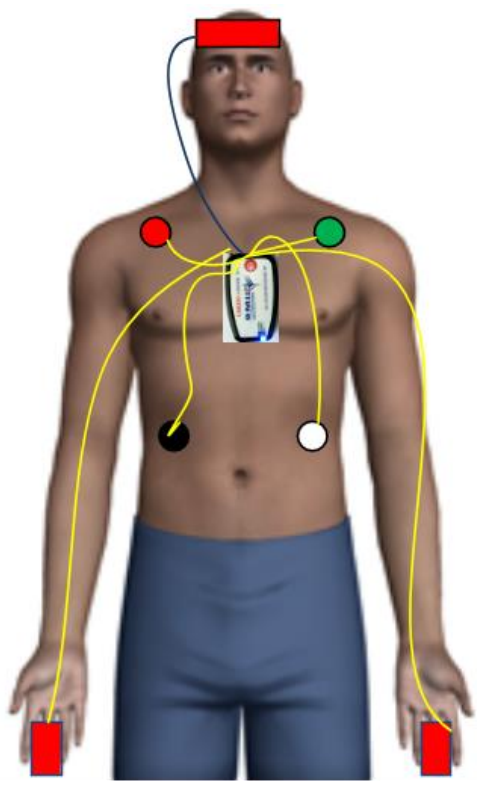

Figure 3.1: CardioHolter electrodes positioning.

The CardioHolter (Figure 3.1) is a monitoring device that combines ECG and PPG technology to provide a comprehensive picture of the wearer's cardiovascular health. Developed by the Kaunas Institute of Technology Biomedical Engineering Institute in Lithuania, the device is designed for monitoring of cardiac conditions. However, this device is bulky with finger PPG and needs to be linked to a computer during the acquisition.

Since 2013, the CardioHolter has been used by Lund University to lead several clinical investigations such as: “Health effects on humans of emissions from vehicles operated with biodiesel” [24]. It is also mainly used by the Biomedical Engineering department in LTH to lead several studies on heart pulses and blood pressure.

On this device are 3 ECG leads and one reference lead measured at a sample rate of 500 Hz. The ECG electrodes are placed on the torso (Figure 3.1). There are also 2 PPG leads (one on each index finger). Those sensors measure the transmission of both red light (635 nm) and infra-red light (960 nm) emitted by LEDs at a sample rate of 250 Hz.

For the data handling, the device’s SD card must be plugged in the computer and the corresponding .DAT file downloaded. A python script gathers the interesting information: the ECG values, the PPG values and their timetables. It is important to note that before being modified, timestamps are the numbers of seconds from 07:00 the same day (so 25 200 seconds are added to have coherent values). This script extracts an array (2 x number of steps for the ECG acquisition)

with the ECG values and their associated timestamps and an array (2 x number of steps for the PPG acquisition) with the PPG values and their associated timestamps.

For the CardioHolter, the measurement has been taken with an acquisition frequency of 250 Hz for the finger ppg and 500Hz for the ECG and an acquisition time around 7 minutes.

3.1.2 Empatica Embrace +

Figure 3.2: Empatica Embrace +.

Empatica is an Italian technology company that specializes in the development of wearable health monitoring devices. Empatica's flagship product is the Embrace + to measure a range of physiological parameters. The company's focus on PPG technology is driven by the belief that it offers a more user-friendly and accessible alternative to traditional medical monitoring devices.

The Empatica Embrace + (Figure 3.2) is a wearable health monitoring device that uses PPG technology to measure various physiological parameters of the wearer. It is a sleek, wrist-worn device that can track and monitor heart rate, blood oxygen levels, skin temperature, and even changes in electrodermal activity (EDA).

The Embrace + is designed to be easy to use and comfortable to wear. It features a simple, intuitive interface. The device is also water-resistant, making it suitable for use during physical activities such as swimming or running.

This wristband device has one PPG lead and a battery life of 7 days. The sensor measures the reflectance of green light (530 nm), red light (655 nm) and infrared light (940 nm) emitted by LEDs at a sample rate of 64 Hz. The hardware manipulation is simple as the watch only has 2 buttons. It is connected to a smartphone and easily usable with the Empatica Care application.

The Empatica data is stocked online on an AWS server in a .avro file. It can be gathered using an external application such as Cyberduck. The desired tables provided are the PPG values, the acquisition

frequency, the start time, the accelerometer values and the systolic peaks' table. The timetable is generated using the start time and the acquisition frequency. This script extracts an array (2 x number of steps for the PPG acquisition) with the PPG values and their associated timestamps, an array (2 x number of steps for the accelerometer acquisition) with the accelerometer values and their associated timestamps and an array (1 x number of systolic peaks) with the peak's associated timestamps.

For the Empatica Embrace + wristband PPG, the measurement has been taken with an acquisition frequency of 64 Hz and an acquisition time around 5 minutes.

3.1.3 Bittium eMotion Faros

Figure 3.3: Bittium eMotion Faros 360.

Bittium is a Finnish technology company that specializes in the development of advanced wireless communication and medical technology solutions. Bittium's medical technology division focuses on the development of advanced monitoring and diagnostic devices, including the Faros 360 ECG device. The company's expertise in wireless communication and sensor technology has allowed it to create devices that are both highly accurate and user-friendly.

The Bittium Faros 360 (Figure 3.3) is a portable electrocardiogram (ECG) device that offers a range of advanced features for monitoring and analyzing the wearer's heart function. The device is designed to be easy to use and comfortable to wear, making it ideal for long-term monitoring of cardiac conditions.

The Faros 360 features a compact, lightweight design. The device uses advanced ECG technology to capture high-quality signals from the heart, even in noisy or challenging environments.

The device features a long battery life, with up to 48 hours of continuous monitoring on a single charge. It is compatible with a range of software applications for data analysis and can be used in clinical settings or for remote monitoring of patients.

On this device are 3 ECG leads measured at a sample rate up to 1 kHz. As the Empatica wristband, it has a battery life of 7 days. The ECG electrodes are, for this device as for the CardioHolter, placed on the torso.

The hardware manipulation is extremely simple because the device only has one button to turn it on and off.

The Faros data is stored on the device and is gathered by plugging the device to a computer and downloading an .EDF file. The frequency is known as it is chosen before the acquisition. As for the Empatica data, the timetable is generated using the frequency (hard coded into the script). This script extracts an array (2 x number of steps for the ECG acquisition) with the ECG values and their associated times.

For the Faros ECG acquisition, electrodes are also placed on the torso. The acquisition frequency is 1000 Hz, and the acquisition time is approximately 5 minutes.

3.1.4 Data Acquisition

For this thesis, the data has been acquired simultaneously on the three devices on one volunteer. The recordings last from 5 minutes to 1h and at rest.

The data acquisition is not the same depending on each device. As the purpose of this thesis is to develop a tool for the Biomedical Engineering Department, a manual (Figure 3.4) has been written to synthesize each step of the acquisition process.

For the CardioHolter, the hardware manipulation is then very basic and the software manipulation intuitive. The clock is the same as the one of the computer linked to the device during the acquisition and is the same for the ECG and PPG recordings.

When worn correctly, the Empatica watch is easy to handle and does not impact on any motion. The clock is connected to the smartphone's one.

For the Faros device, both the hardware and the wires are less bulky than for the CardioHolter. The software allows a choice in the frequency of acquisition, the file format and several parameters such as the temperature and the channel count. Those parameters are entered on the software which opens when plugging the device to a computer. The device clock is linked to the computer clock.

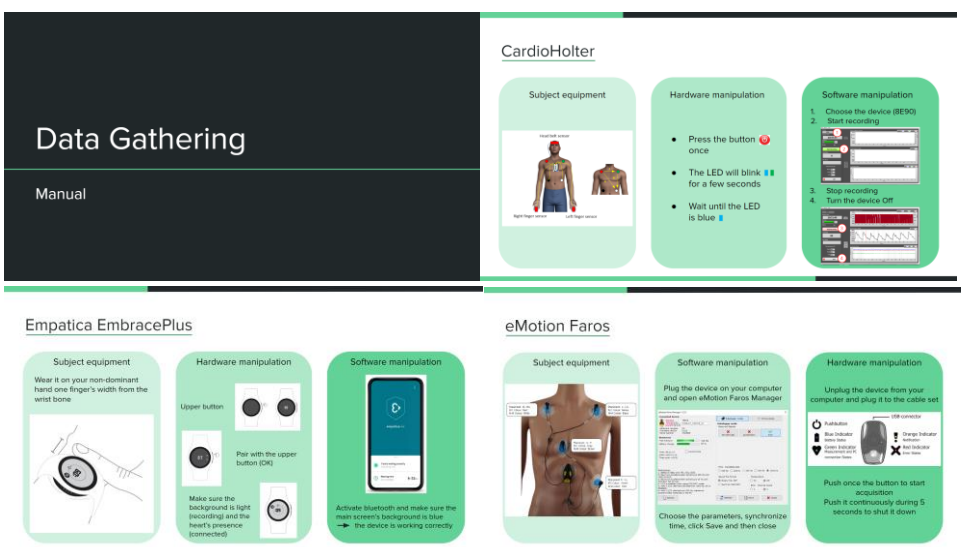

Figure 3.4: Data Gathering Manual.

3.1.5 Data Handling

Once acquired, the data needs to be gathered before being exploited. We want to have a unique way to exploit the data and count the time that is the number of seconds from 00:00 the same day.

As the purpose of this thesis is to develop a tool for the Biomedical Engineering Department, a manual (Figure 3.5) has been written to synthetize each step of all the data treatment process.

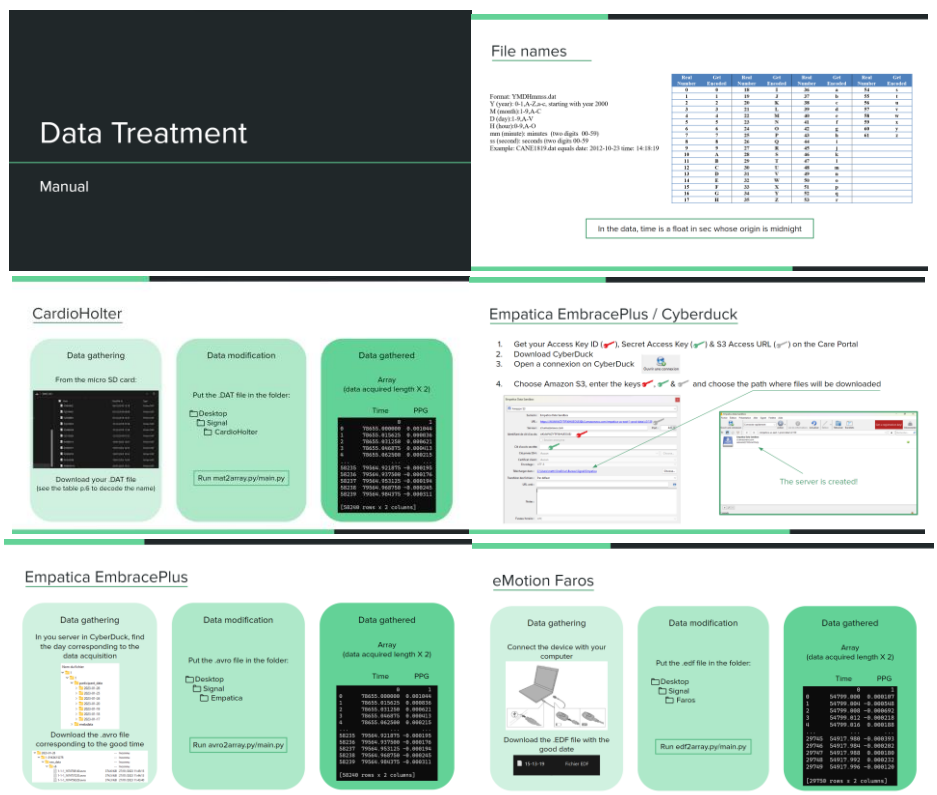

Figure 3.5: Data Treatment Manual.

3.2 Processing

Once the data is acquired and handled in a usable format, we exploit it to analyze its characteristics.

3.2.1 Heart Rate

As seen in section 2.2, the heart rate is a conversion of the lag between two consecutive pulses and a peak detection is mandatory to measure the heart rate.

3.2.1.1 Peak Detection

The point of detecting the peak of a pulse is to get for each pulse the timecode of a very specific point. Several methods exist depending on the waveform.

For ECG signals (Figure 3.6), peaks are extremely thin and with a high amplitude, making their detection simple with a high precision. Indeed, the R wave's amplitude is about 4 times higher than the T peak's one and 10 times higher than the P peak's one for a width of 0.03 s whereas it is around 0.05 s for the P wave and 0.2 s for the T wave.

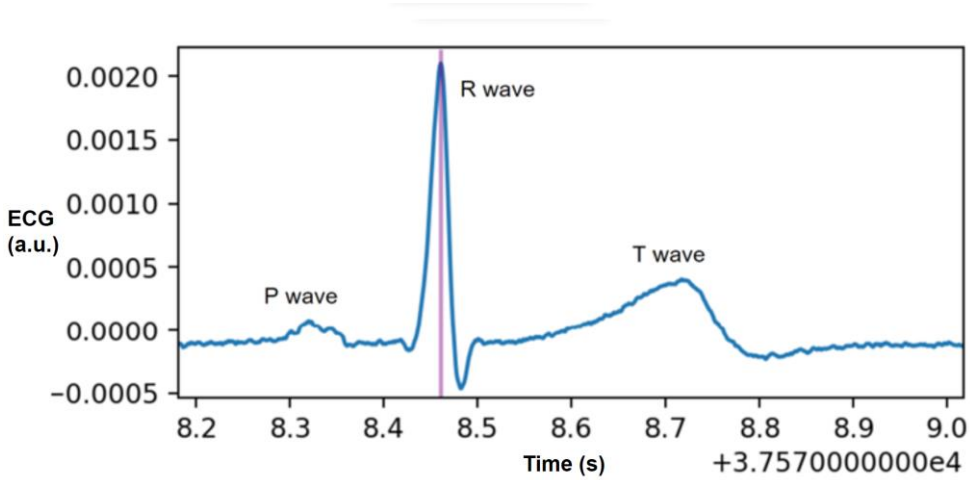

Figure 3.6: One ECG peak.

Using these properties, we detect each peak of the ECG signal by detecting each maximum of the signal and excluding the ones that do not reach a certain percentage of the R wave maximum. In the following signals (Figure 3.7), peaks were selected for an amplitude of 50% of the maximum amplitude on a 5 s time range.

This ECG peak detection is a simplified and self-computed version of the Pan-Tompkins algorithm [25]. Indeed, the choice has been here to consider the raw signal as clean (as it has been acquired at rest) and the parameters excluding “false peaks” (detection of peaks where there should not be any) are specially chosen to fit with the raw ECG signals after adjustments.

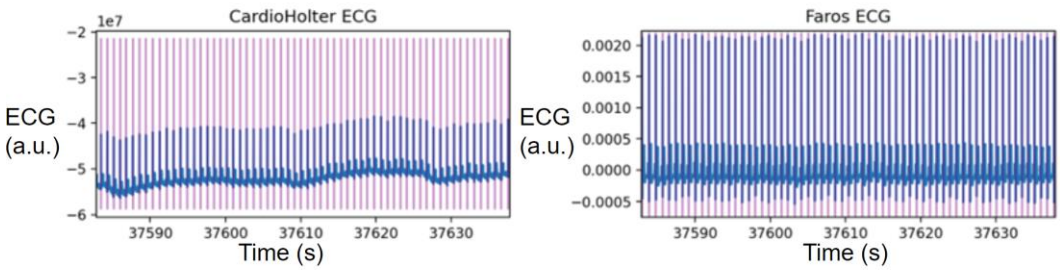

Figure 3.7: ECG peak detection for the CardioHolter and Faros devices and for approximately 50 s.

For PPG signals (Figure 3.8), peaks are less detectable. Indeed, the systolic peak is quite large in time (around 0.6 s) and does not always have a precise peak. Furthermore, the difference between its amplitude and the diastolic peak's amplitude is not that consequent (the diastolic peak's amplitude is 30-70% of the systolic peak's amplitude) so the peak selection could unintentionally include diastolic peaks or exclude systolic peaks.

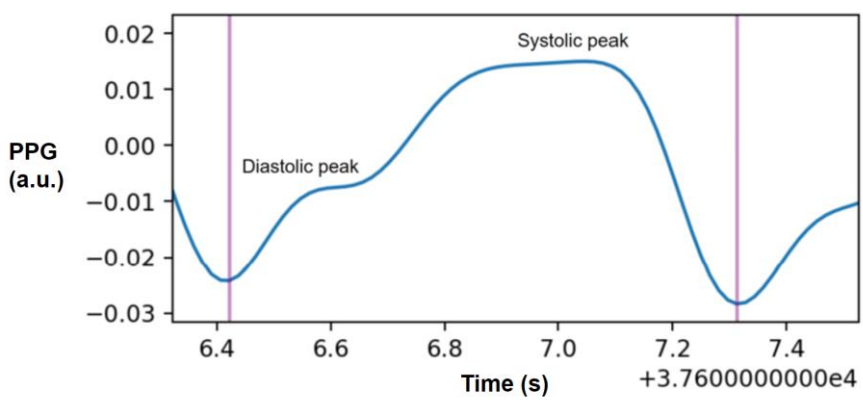

Figure 3.8: One PPG pulse.

Several methods exist for the PPG peak detection. Three methods have been tested. The first one is the detection of the points having the value 50%($max_{PPG} - min_{PPG}$) [26]. However, this method was not chosen as it needs the detection of the maximum up-slope of the pulse and the minimum of the pulse. The second method is the detection of the maximum up-slope of the pulse [11]. According to the pulse waveform, the method which seems to be the most precise and simplest way to detect a characteristic point of the pulse is the negative peak detection. Indeed, it is thinner than the systolic peak (less than 0.3 s) and more importantly has a well-defined peak in opposition to the systolic peak (or even the diastolic peak).

The PPG peak selection cannot use the same criteria as the ECG signal peak detection because there are more variations of the amplitude over time. So, another criteria is used with the following signals (Figure 3.9): the minimum time gap between two consecutive peaks (0.3 s corresponding to 200 bpm) [27].

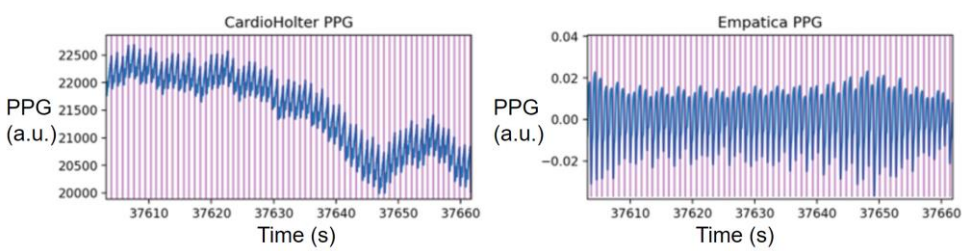

Figure 3.9: PPG peak detection for the CardioHolter and Empatica devices and for approximately 60 s.

3.2.1.2 Time Synchronization

The main advantage of the CardioHolter device is the perfect synchronization for both ECG and PPG signals as they are both measured by the same device, with the same internal clock. On the other hand, the Faros device and the Empatica device are not initially synchronized and have 2 different internal clocks. The Empatica uses the clock of the smartphone, which the device is paired with, and the Faros uses the one of the computer on which the Faros settings are managed.

As we are interested on the pulse transit time and its variability between the Faros ECG signal and the Empatica PPG signal, the clocks of the two devices must be synchronized. It is consequently very important to have a precise idea of the lag between both signals.

The first explored idea was to pretend that this lag is less than the time between two pulses. So, it could be simply calculated with the subtraction: $t_{PPG\_peak} - t_{ECG\_peak}$. However, using this method, the lag was too variable and there was a time lag between the PPG HR curve and the ECG one.

To know the lag between both signals, the signals from the different devices are unfortunately too different to allow the comparison of raw signals (the CardioHolter ECG with the Faros ECG and the CardioHolter PPG with the Empatica PPG). So, the solution has been to shift the Faros ECG HR curve time step by time step and

calculating the correlation of this curve with the Empatica PPG heart rate curve.

As the lag consistency is studied, several acquisitions are made (7 in total) in the exact same conditions (at rest, on the same participant, with the electrodes at the same positions and for the same acquisition time). The lag is then computed for each acquisition.

3.2.1.3 HR Computation

The heart rate is obtained in two steps:

First, we calculate the instantaneous heart rate. This value is called d_{HF} (Figure 3.10):

$$d_{HF}(t_i) = \frac{1}{t_i - t_{i-1}} \tag{3.1}$$

t_i is the time for the ith peak and $t_{i-1}$the time for the i-1th peak.

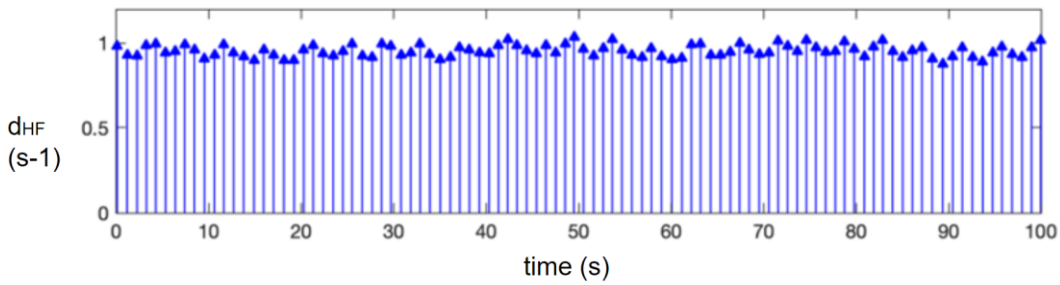

Figure 3.10: d_{HF} computation.

Then we interpolate the d_{HF} list and multiply it by 60 to have an HR in beat per minute (bpm) (Figure 3.11).

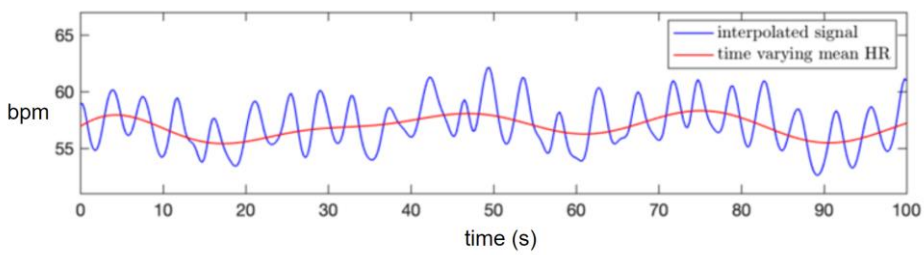

Figure 3.11: HR and mean HR computation.

3.2.1.4 HRV Computation

We use the same method as Youna Marc-Derrien's thesis [28] to compute the HRV (Figure 3.12). It consists in subtracting the time-varying mean HR from HR. The HRV value is, as the HR, in bpm.

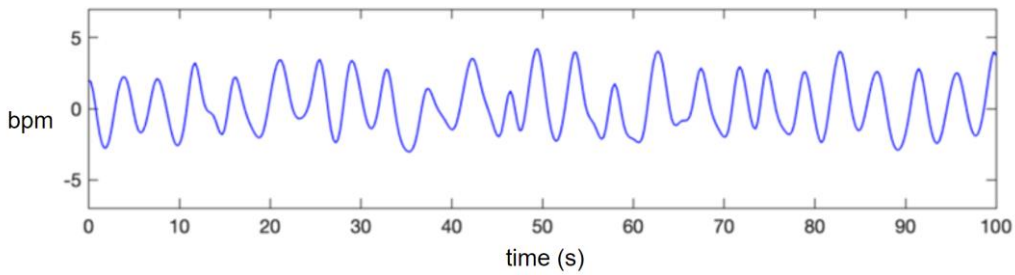

Figure 3.12: HRV computation.

The SDRR, RMSSD, LF and HF metrics are defined by the following formulas.

The standard deviation of the RR interval formula is:

$$SDRR = \sqrt{\frac{\sum_{i=1}^{N}(RR_i - \mu)^2}{N}} \tag{3.2}$$

With RR_i the i^{th} RR interval, N the number of RR intervals and μ the mean of all the RR intervals.

The root mean square of successive RR interval differences formula is:

$$RMSSD = \sqrt{\frac{\sum_{i=2}^{N}(RR_i - RR_{i-1})^2}{N-1}} \tag{3.3}$$

LF power represents the power in the low-frequency range, from 0.04 Hz to 0.15 Hz. It is obtained by integrating the power spectral density (PSD) within the defined low-frequency range.

HF power represents the power in the high-frequency range, from 0.15 Hz to 0.4 Hz. It is obtained by integrating the power spectral density (PSD) within the defined high-frequency range.

3.2.2 PTT Computation

The PTT computation for each signal is simple once the peaks are detected on both ECG and PPG signals. However, this can only be done if we are sure that the ECG and PPG signals are synchronized.

The pulse transit time in our study is the lag for the same pulse: $t_{PPG\_peak} - t_{ECG\_peak}$ (Figure 3.13). It represents the transit time of the pulse from the torso to the wrist (when measured by the Empatica device) or the finger (when measured by the CardioHolter). But the peaks detected do not represent the same point of the pulse, as ECG and PPG pulses do not have the same waveform. Consequently, what will interest us is the consistency of the PTT and the comparison of the PTT values for the CardioHolter and for the association Faros and Empatica. So the PTT is computed for each pulse by calculating the time ECG device position – PPG device position in the body and the comparison of the CardioHolter PTT with the Faros-Empatica combination PTT will be compared in their consistency and main values.

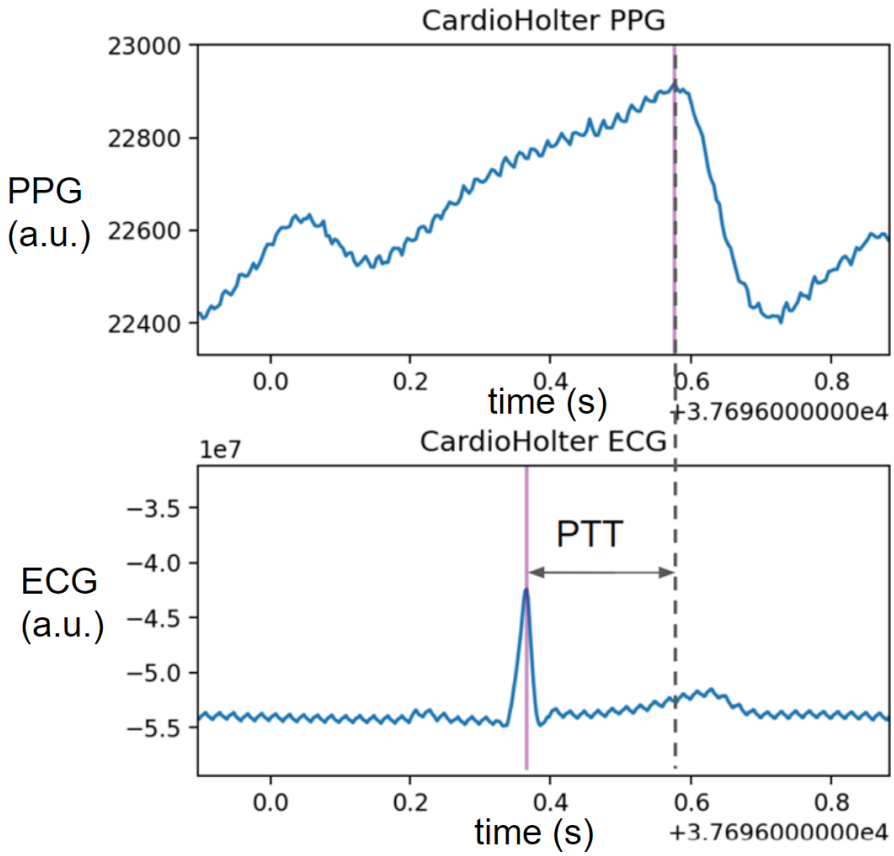

Figure 3.13: PTT computation.

3.2.3 Pulse Decomposition

Once the PPG pulse is isolated, we want to analyze its waveform by decomposing it in a sum of Gaussian functions. A Gaussian function is defined by the following formula [29]:

$$f(x) = A \exp\left(-\frac{(x-m)^2}{2\sigma^2}\right) \tag{3.4}$$

Two methods [19] are explored for the decomposition and will be compared by an analysis of the correlation between the pulse from the raw signal and the sum of the Gaussians decomposing it. The correlation analysis is computed with two methods (3.2.1.2 and 3.1.2.3).

3.2.3.1 Pulse Decomposition

The PPG pulse is decomposable in a sum of Gaussian functions as seen in part 2.4. For that, it is important to first identify and extract each pulse from the raw signal.

The pulse identification (Figure 3.14) is performed by detecting the peak of a pulse and including the signal for a certain amount of time before and after the peak. In this study, the Empatica PPG pulses are selected with a beginning at the negative peak (part 3.2.1.1) and a duration of 0.8 s. The CardioHolter PPG pulses have another

reference which is the maximum peak. The peak detection is based on this reference and the pulses are shifted in time. The maximum peak time mean has been calculated and is 0.68 s after the beginning of the pulse so the pulse is shifted with 0.68 s before the peak and the duration of the pulse is 0.8 s.

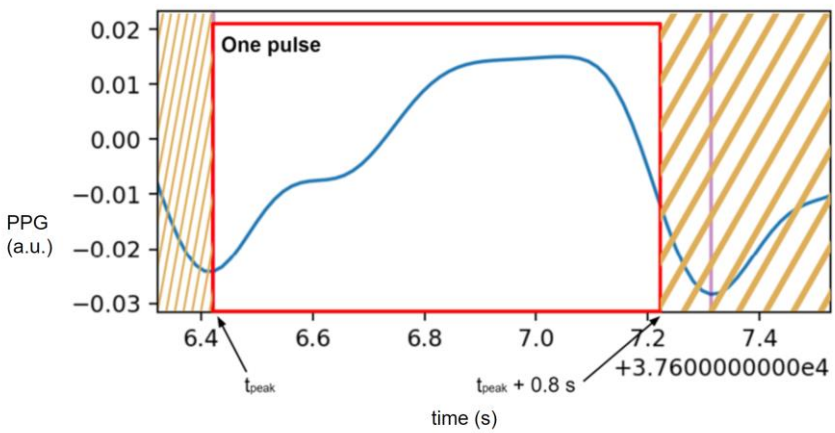

Figure 3.14: Computation of the identification of one pulse.

Then, the offset of each pulse is cancelled to have a quantity of pulses as similar as possible. As a representative pulse is wanted to be analyzed, all the Empatica pulses are averaged and the median average pulse is chosen for the decomposition. The equivalent pulse from the CardioHolter PPG signal is decomposed.

The first method is the decomposition of the whole pulse in a certain number of Gaussians. I chose to decompose it in 3 Gaussians (Figure 3.15), as it is how it was done for the CardioHolter PPG in Youna Marc-Derrien's thesis [19].

- The first step is to find the Gaussian (Gaussian G0) with the highest correlation coefficient (with A, σ and m optimized from equation 3.2) for the initial pulse (P0).
- This Gaussian is kept and subtracted from (P0) to have a modified pulse (P1).
- The Gaussian (Gaussian G1) with the highest correlation coefficient with (P1) is calculated and subtracted from (P1) to obtain (P2).
- The Gaussian (Gaussian G2) correlating the most with (P2) is calculated.
- Then, (P0), (P1) and (P2) are added to fit with the initial pulse (P0).

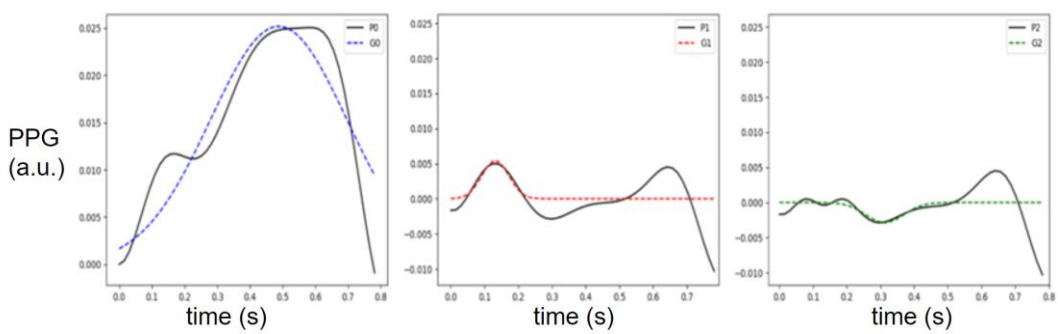

Figure 3.15: Pulse decomposition in 3 Gaussians step by step.

The second method (Figure 3.16) uses a split of the initial pulse (P0) in two parts ($P0_{left}$) and ($P0_{right}$). This split occurs at the minimum point between the systolic and the diastolic peaks.

- It first decomposes the first part ($P0_{right}$) in two Gaussians ($G0_{right}$) and ($G1_{right}$) using the same steps as the first method.
- Then the continuation of ($G0_{right}$) and ($G1_{right}$) on the left part are subtracted from ($P0_{left}$) to get ($P1_{left}$).
- Finally, ($P1_{left}$) is decomposed in two Gaussians ($G0_{left}$) and ($G1_{left}$) and all the Gaussians are added to fit with the initial pulse.

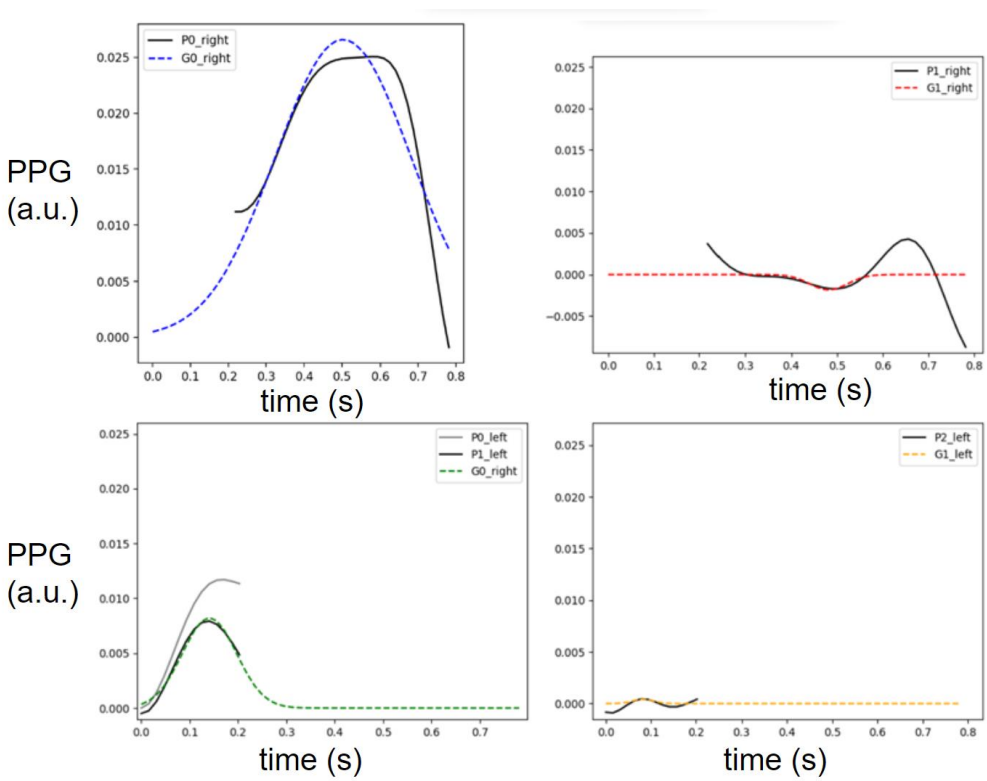

Figure 3.16: Pulse split in 2 pulses and decomposition of each pulse in 2 Gaussians step by step.

3.2.3.2 Goodness of fit – Mean Absolute Error

The first method uses the Mean Absolute Error (MAE) to quantify goodness-of-fit for the modeled PPG pulse. It is defined by the following formula [30]:

$$MAE = \frac{1}{n}\sum_{i=1}^{n}\left|X_{original}(i) - X_{computed}(i)\right| \quad (3.5)$$

With n the number of points constituting the pulse, $X_{original}$ the original pulse and $X_{computed}$ the sum of the Gaussian functions decomposing the pulse.

We will in our study compute the percentage of correlation between the inner curve and its decomposition with the formula:

$$MA_{\%} = 100 - \frac{MAE}{\frac{1}{n}\sum_{i=1}^{n}\left|X_{original}(i)\right|} \quad (3.6)$$

3.2.3.3 Goodness of fit – Root Mean Square Error

The second method uses the Root Mean Square Error (RMSE) to quantify goodness-of-fit for the modelled PPG pulse. It is defined by the following formula [30]:

$$RMSE = \sqrt{\frac{1}{n}\sum_{i=1}^{n} e_i^2} \tag{3.7}$$

With the same parameters as for the MAE.

I will in my study compute the percentage of correlation between the inner curve and its decomposition with the formula:

$$RMS_{\%} = 100 - \frac{RMSE}{\frac{1}{n}\sum_{i=1}^{n}\left|X_{original}(i)\right|} \tag{3.8}$$

4 Results

4.1 Devices Signals

4.1.1 CardioHolter PPG

The CardioHolter finger PPG waveform (Figure 4.1 & 4.2) has a characteristic shape with distinct peaks and notches that reflect various aspects of cardiovascular function. However, there are baseline variations during the whole acquisition time and the signal contains high frequency noise.

As seen in the background part (2.1.1), the finger PPG waveform is characterized by an initial sharp peak followed by a dicrotic notch and a small secondary peak. The waveform then descends gradually before returning to the baseline.

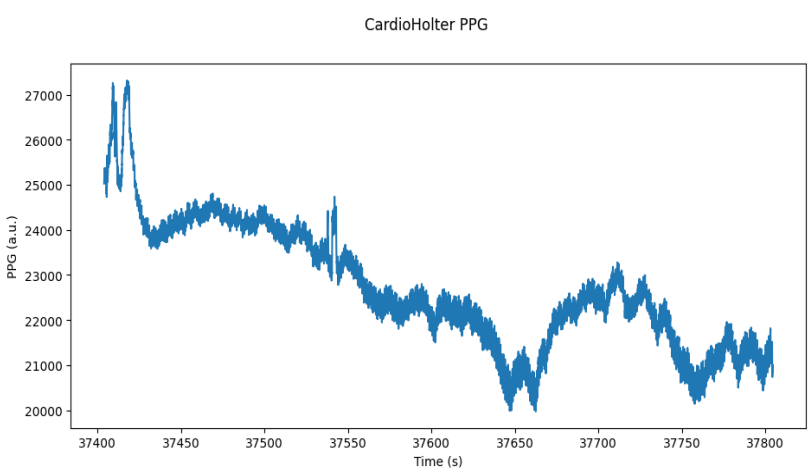

Figure 4.1: CardioHolter PPG signal for a 7-minute acquisition.

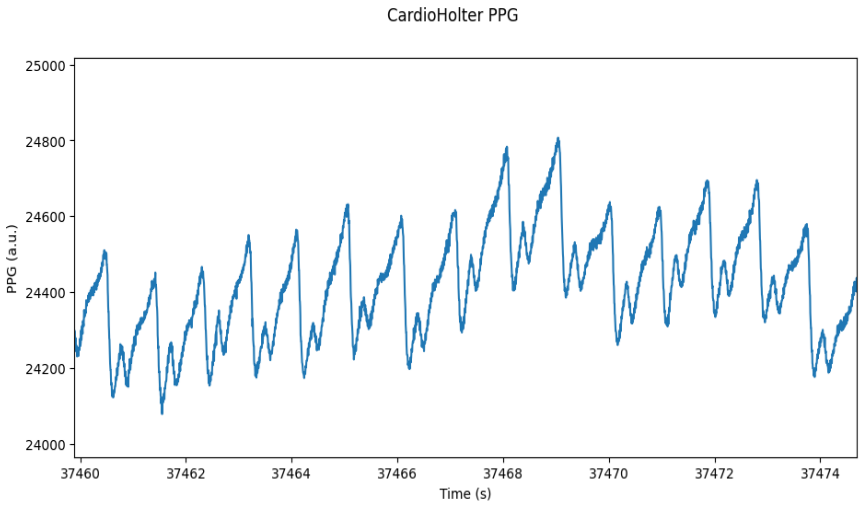

Figure 4.2: CardioHolter PPG signal zoomed on a 15 s slot.

4.1.2 Empatica PPG

Compared to the CardioHolter PPG signal, the mean value of the Empatica PPG signal is stable. The general shape (Figure 4.3 & 4.4) is similar to the CardioHolter one, with an initial sharp peak (percussion wave) and a lightest secondary one (tidal wave). Moreover, the signal is particularly less noisy than the CardioHolter one.

However, the peaks are less sharp for the reflected PPG signal than for the transmitted signal. This is a concern for the exact value of peak times. This is why we will have an interest in negative peaks, that are sharper, for the peak detection.

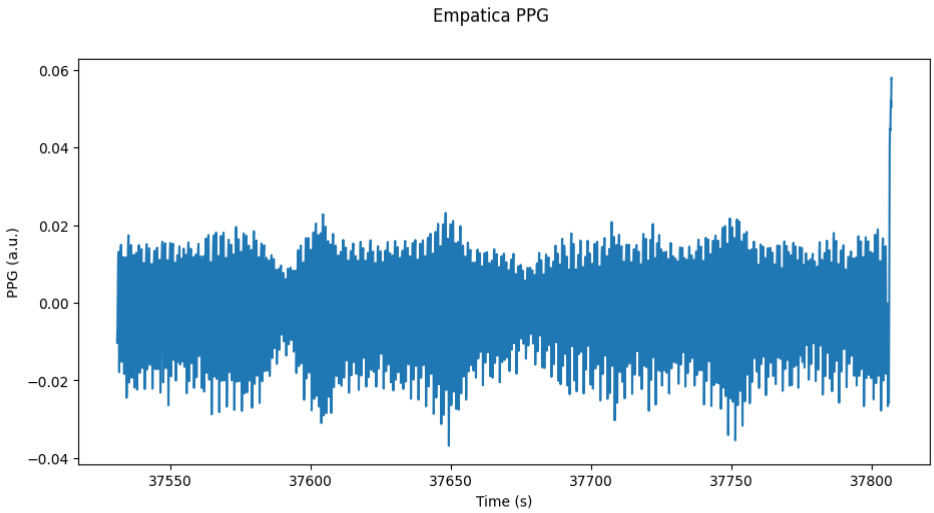

Figure 4.3: Empatica PPG signal for a 5-minute acquisition.

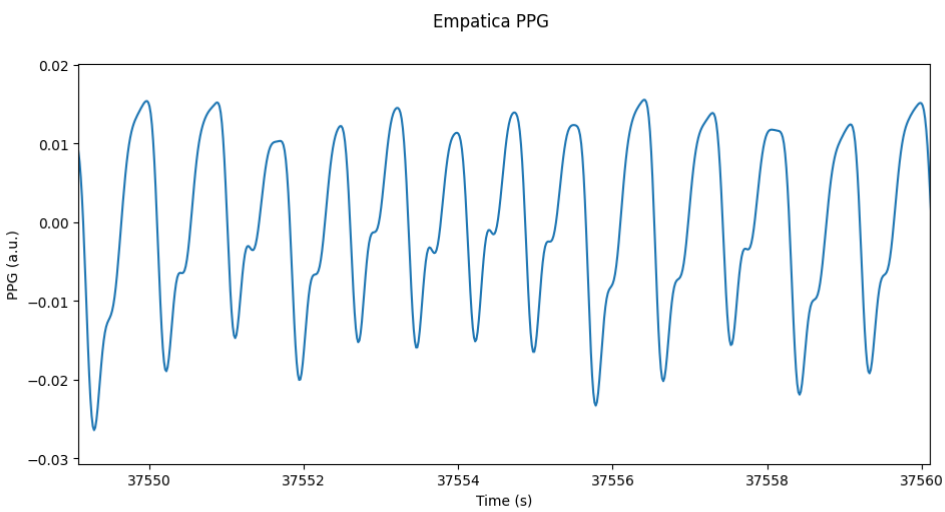

Figure 4.4: Empatica PPG signal zoomed on a 15 s slot.

4.1.3 CardioHolter ECG

Even if it is less than for the PPG signal, the main ECG signal value is variable during the whole acquisition time and is lightly noisy. However, when focusing on a few seconds, the signal (Figure 4.5 & 4.6) exhibits a significant level of periodicity.

The characteristics of ECG signals are recognizable on this device's signal: a thin P wave and a quite sharp T wave are identifiable. The QRS complex is extremely sharp, this an important point for the peak detection in the pre-processing.

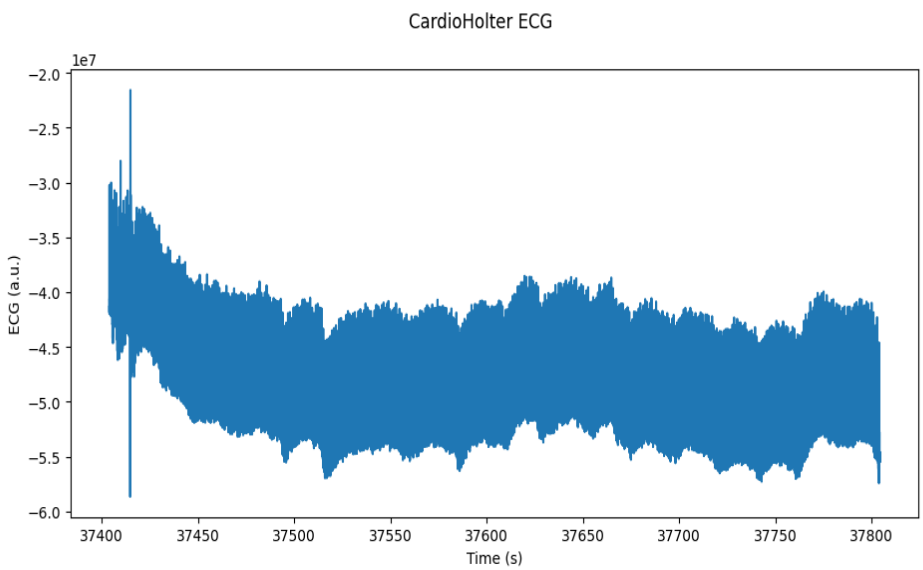

Figure 4.5: CardioHolter ECG signal for a 7-minute acquisition.

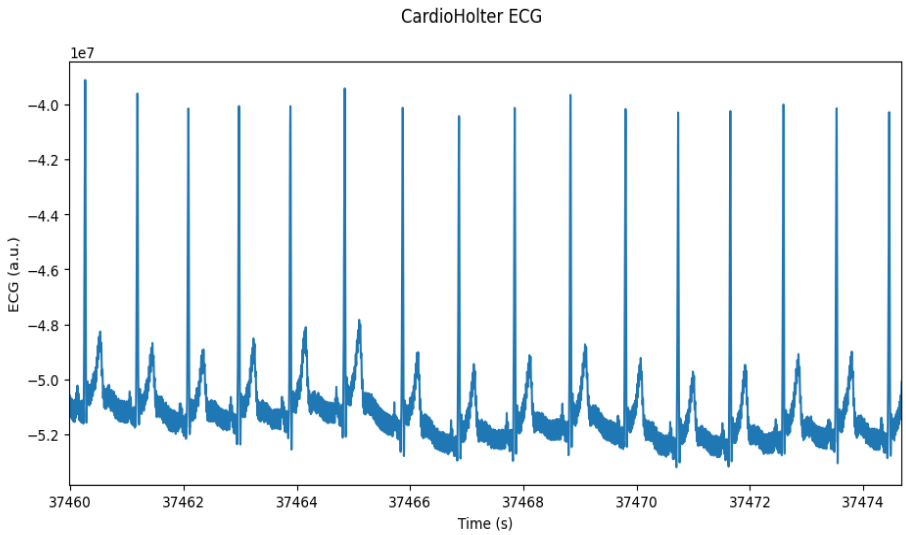

Figure 4.6: CardioHolter ECG signal zoomed on a 15 s slot.

4.1.4 Faros ECG

For the Faros ECG acquisition, the signal has a significant stability during the whole acquisition and almost no noise. The signal is extremely periodical.

The characteristics of ECG signals are even more recognizable on this device's signal (Figure 4.7 & 4.8). The P wave is clearer than the CardioHolter one. The T wave is less noisy and the QRS complex is extremely sharp as for the CardioHolter. The signal is very periodic and its patterns clearly identifiable.

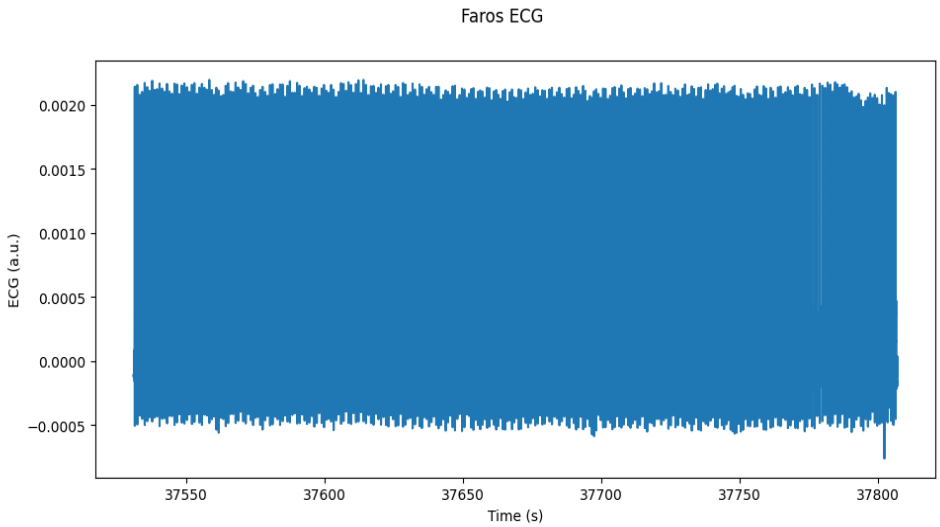

Figure 4.7: Faros ECG signal for a 5-minute acquisition.

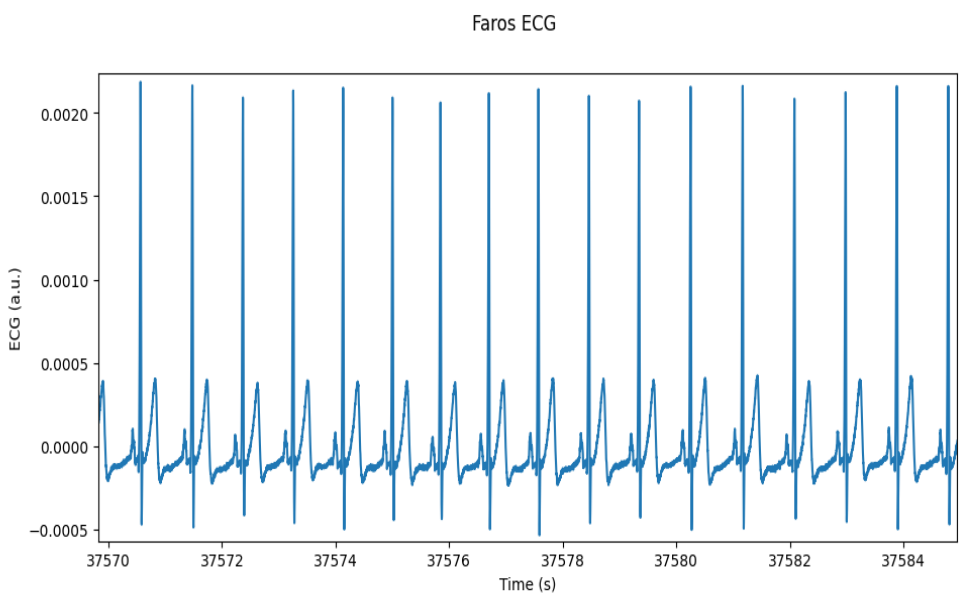

Figure 4.8: Faros ECG signal zoomed on a 15 s slot.

4.2 Signals Comparison

Once the signals acquired, HR, HRV, PTT and pulse decomposition are computed, and those characteristics are analyzed and compared for the CardioHolter and for the combination Empatica/Faros.

4.2.1 Heart Rate

4.2.1.1 Peak Detection

As seen in (3.2.1.1), the HR computation needs to first detect peaks. Both methods (3.2.1.1), minimum and maximum peak detection for the Empatica PPG signal are compared (Figure 4.9).

This comparison shows that the HR computed is noticeably more consistent for the minimum peak detection whereas the HR computed with the maximum peak detection is extremely noisy.

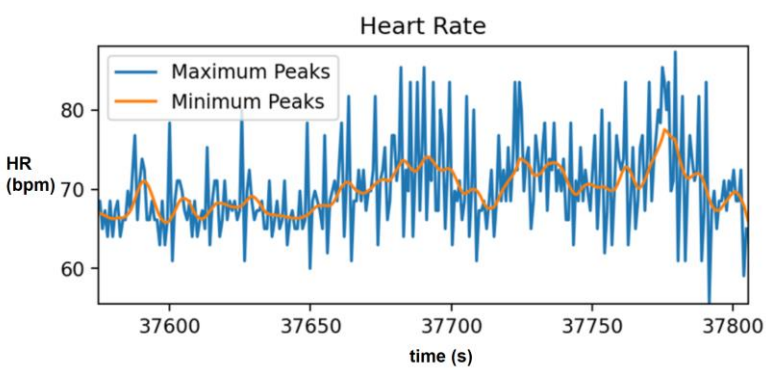

Figure 4.9: Heart rate measured by the Empatica PPG considering the minimum or maximum peaks during peak detection.

4.2.1.2 Time Synchronization

The heart rate being computed, it has been plotted for the 4 signals on the same graph (Figure 4.10). We observe a correct synchronization for 3 signals (CardioHolter PPG and ECG and Empatica PPG) but a consequent lag with the Faros ECG (ECG Faros Uncorr.).

However, the shape of the signal is similar for all signals, even for the Faros ECG, so HR is used for the lag correction detecting the gap for which the correlation coefficient between the Empatica PPG HR signal and the Faros ECG HR corrected signal (ECG Faros corr.) is the highest.

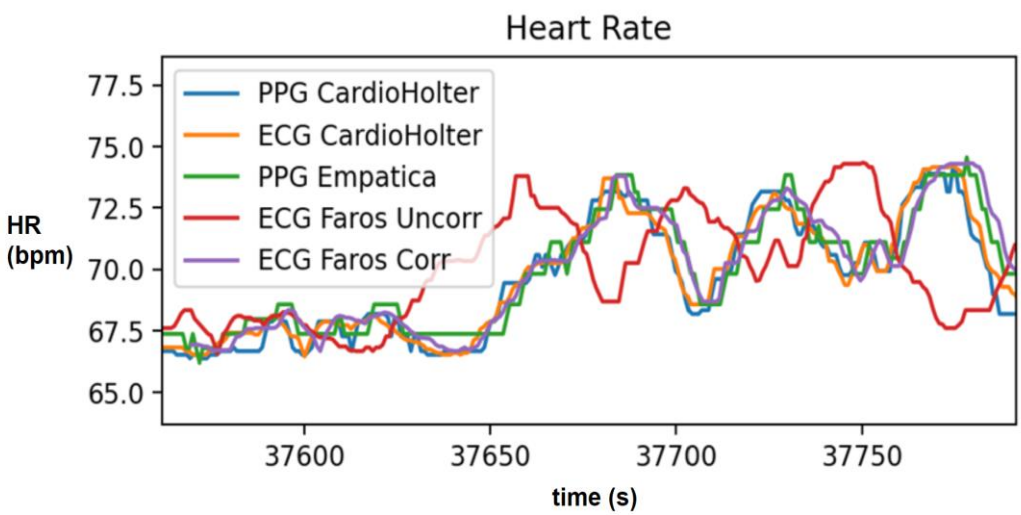

Figure 4.10: Heart rate measured with the 4 signals for 4 minutes.

The lag is computed for each acquisition (Figure 4.11), following the 3.2.1.2 protocol to have an idea of its consistency.

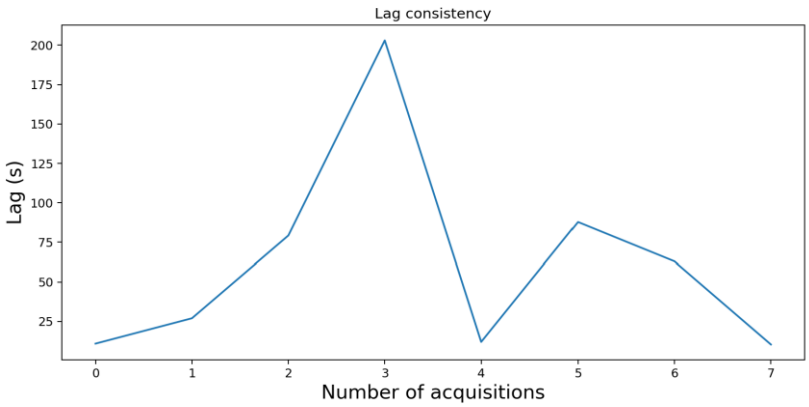

Figure 4.11: Faros signal lag consistency over acquisitions.

Unfortunately, the lag between the Faros signal and the Empatica signal is not consistent at all. This is a serious problem for the PTT computation (4.2.2).

4.2.1.3 Heart Rate

Using the previous results, HR is computed with the maximum peak detection for the CardioHolter ECG and PPG and the Faros ECG signals and with the minimum peak detection for the Empatica PPG signal. Then, the Faros signal is shifted to remove the lag between this signal and the Empatica signal. The HR signals are plotted on Figure 4.12:

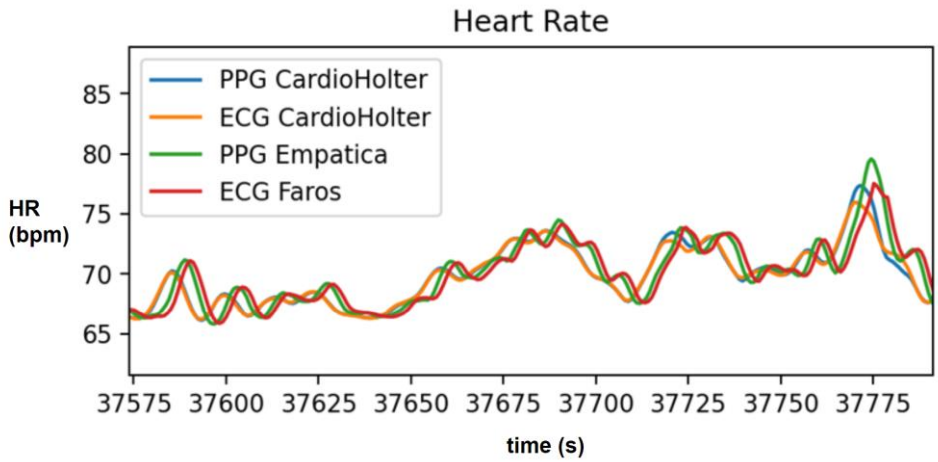

Figure 4.12: Heart rate measured by the for signals for 200 s.

We observe that the HR signals are extremely similar for the CardioHolter and the Empatica/Faros combination (with a slight lag between both HR due to a different internal clock).

We can conclude on the HR analysis that the CardioHolter is replaceable by the Empatica device and the Faros device (as only one device is sufficient for HR) as the computed HR signals are as accurate for all the devices and very similar.

4.2.1.4 Heart Rate Variability

For each HR signal, the time varying mean HR (Figure 4.13) is computed for each acquisition point by averaging the HR values on a 20 acquisition points sliding window.

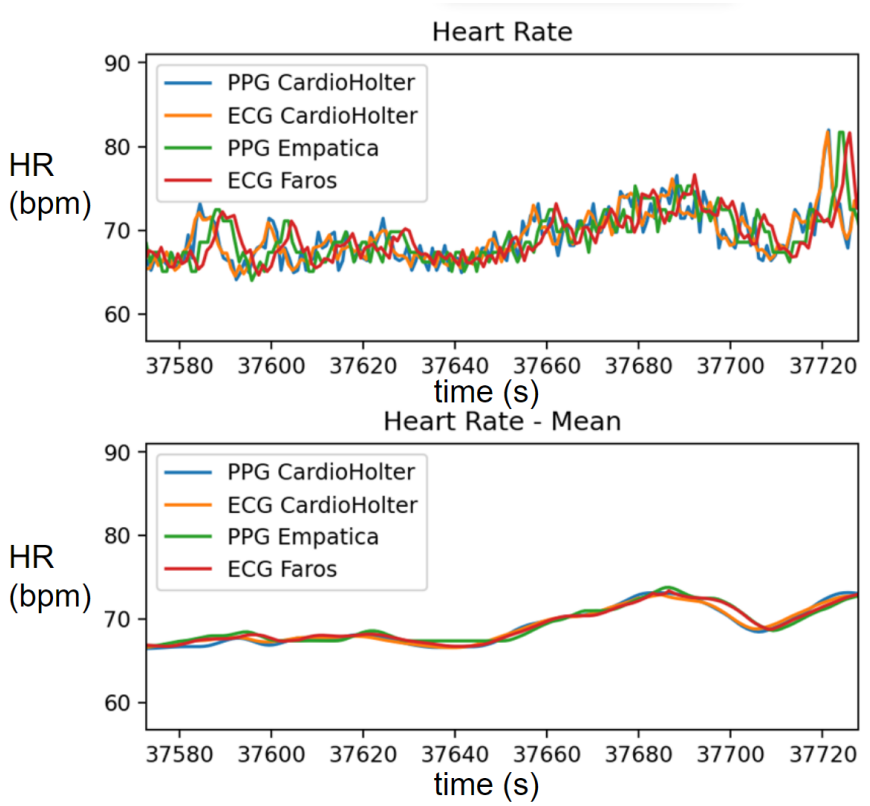

Figure 4.13: Heart rate and time varying mean HR.

The heart rate variability is computed following the (3.2.1.4) method and plotted (Figure 4.14).

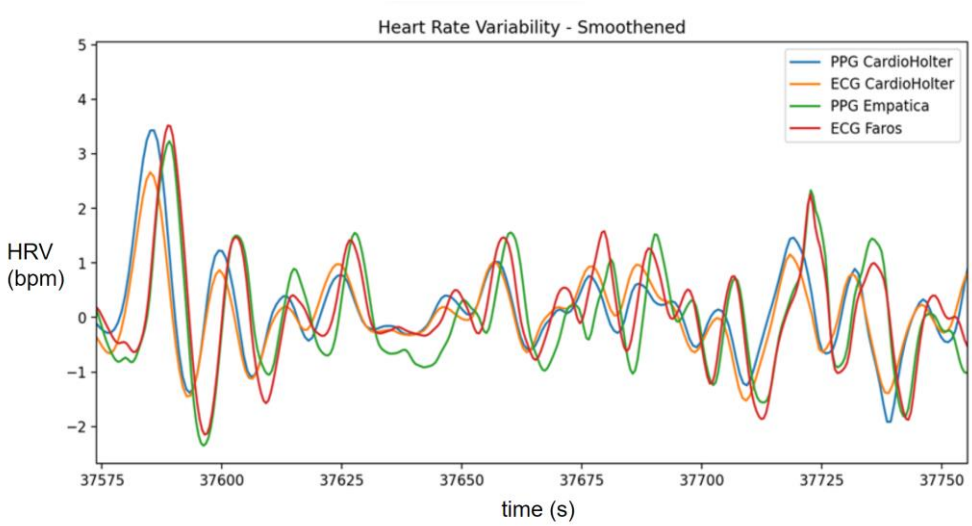

Figure 4.14: HRV computed for each signal.

The graph shows that the Empatica and Faros HRV are very similar and have the same waveform as the CardioHolter HRVs despite the same slight lag as the one observed in HR curves (due to different internal clocks). This is an expected result as HR are very similar and HRV computed after HR. However, the HRV amplitude is slightly higher for the Empatica and Faros signals (between 20 and 40% higher).

The HRV metrics are presented in Table 4.1:

Table 4.1: HRV metrics for the 4 signals, based on the same 3-min recording.

	SDRR (s)	RMSSD (s)	LF (s^2)	HF (s^2)	LF/HF	SDRR/RMSSD
CardioHolter PPG	0,037	0,027	0,00017	0,00011	1,54	1,37
Empatica PPG	0,034	0,025	0,00016	0,00012	1,33	1,36
CardioHolter ECG	0,035	0,023	0,00017	0,00012	1,42	1,52
Faros ECG	0,033	0,021	0,00018	0,00013	1,38	1,57

As for the other results, the ratios the metrics SDRR, RMSSD, LF, HF and their ratios LF/HF and SDRR/RMSSD have an important similarity for all the signals.

4.2.2 Pulse Transit Time

PTT is computed as seen in part 3.2.2. It is extremely consistent for the CardioHolter: the order of magnitude of the PTT variation is 10 ms. The PTT for the combination Empatica/Faros computed when the minimum peaks are detected for the Empatica PPG signal (Figure 4.16) is more consistent (variations of ≈ 200 ms) and has a closer mean value to the CardioHolter one than the PTT computed (Figure 4.15) with the maximum peak detection (variations of ≈ 400 ms).

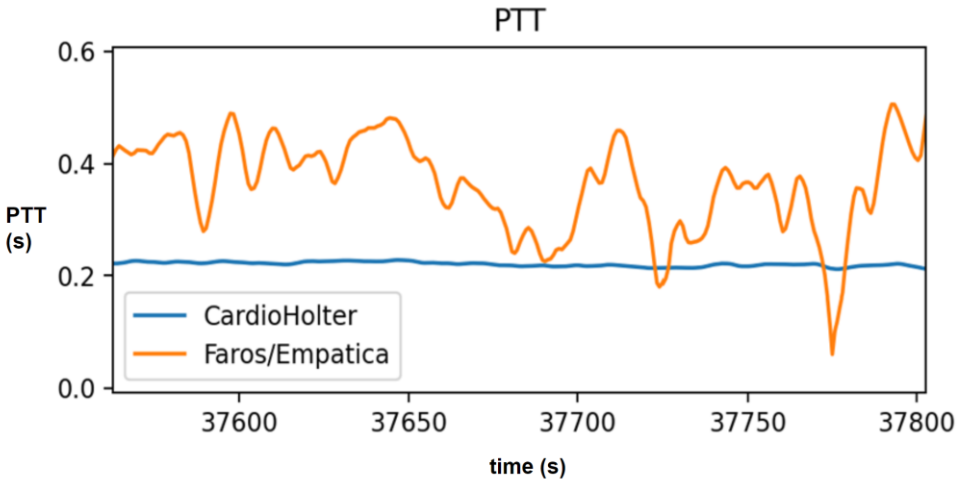

Figure 4.15: CardioHolter and Faros/Empatica PTT when detecting Empatica signal's maximum peaks.

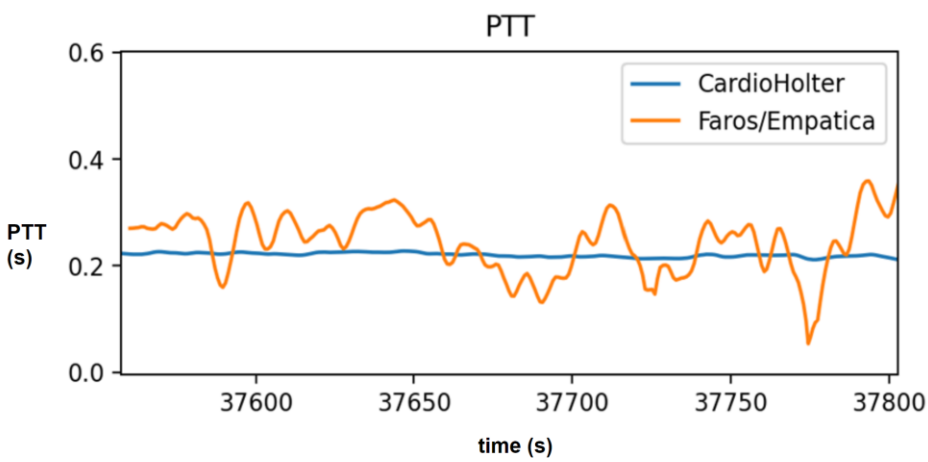

Figure 4.16: CardioHolter and Faros/Empatica PTT when detecting Empatica signal's minimum peaks.

However, the Empatica/Faros PTT computed is not reliable as the Faros signal has been shifted in time. Moreover, this PTT is not satisfying as its variations are 20 times higher than the CardioHolter PTT ones. Consequently, the combination of the Faros and Empatica devices does not allow to compute the PTT between the subject's chest and their wrist.

4.2.3 Pulse Decomposition

The first part of the pulse decomposition is the isolation of each pulse of the Empatica PPG signal (Figure 4.17) and the CardioHolter PPG signal (Figure 4.18).

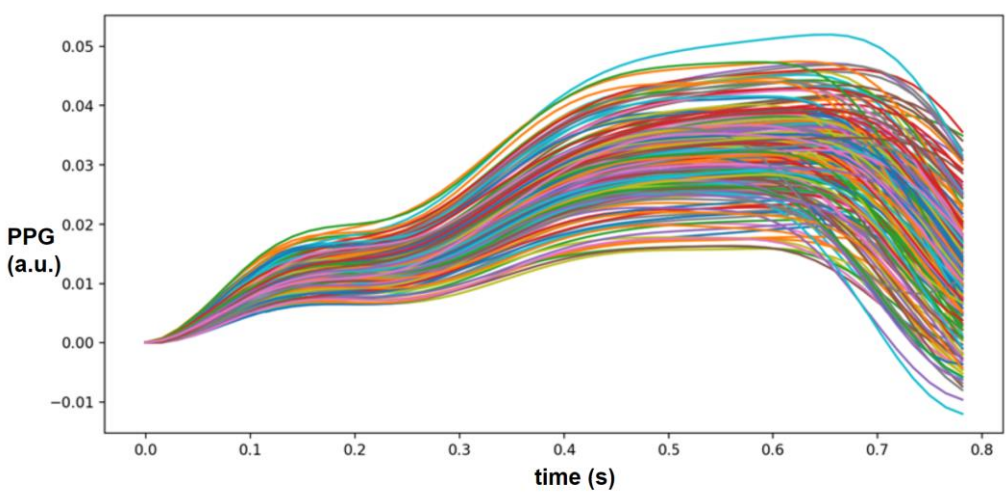

Figure 4.17: Isolation of every pulse in the Empatica PPG signal.

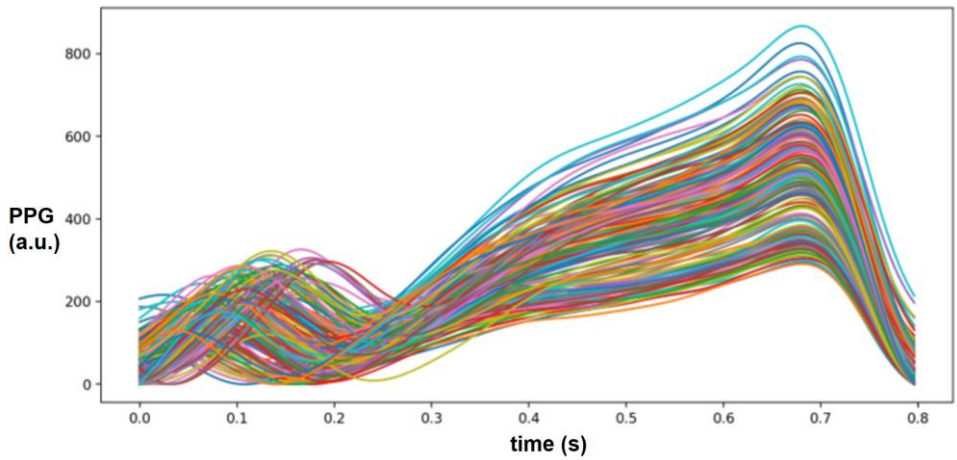

Figure 4.18: Isolation of every pulse in the CardioHolter PPG signal.

As seen in 3.2.3, the pulse is decomposed in a sum of Gaussians by two different ways and the correlation between the Gaussians' sum and the inner curve is computed with two different methods ($MA_{\%}$ and $RMS_{\%}$).

In the first case the Empatica pulse (Figure 4.19) and the CardioHolter pulse (Figure 4.20) are decomposed in a sum of 3 Gaussians (G0, G1 and G2).

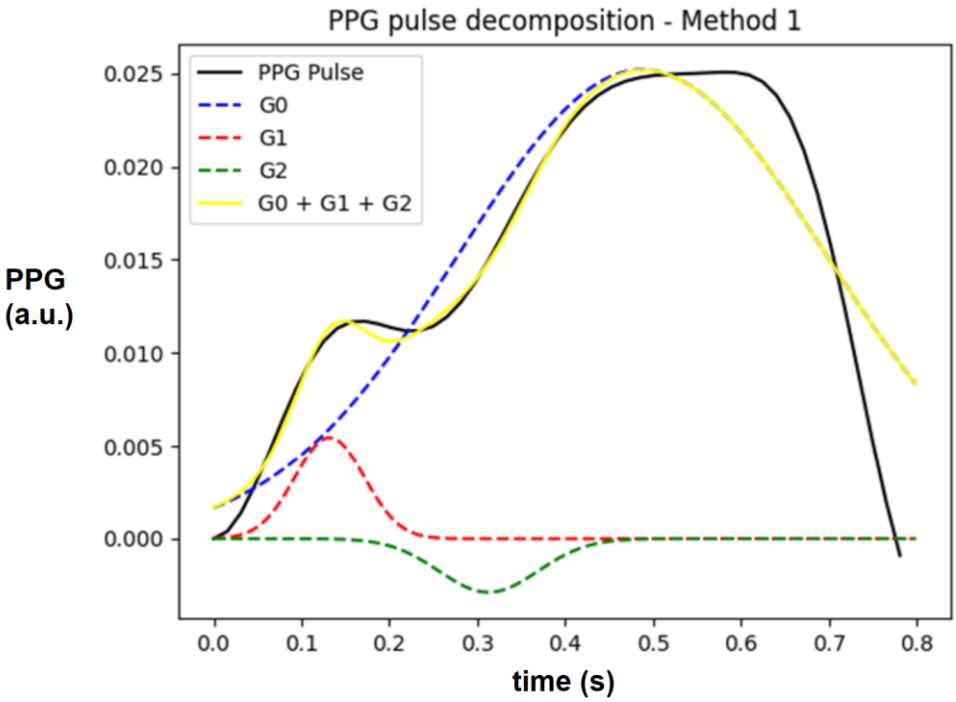

Figure 4.19: Decomposition of the whole Empatica pulse in a sum of 3 Gaussians.

The goodness-of-fit for the modelled pulse is for the Empatica:

$MA_{\%} = 90.26\%$ and $RMS_{\%} = 82.91\%$

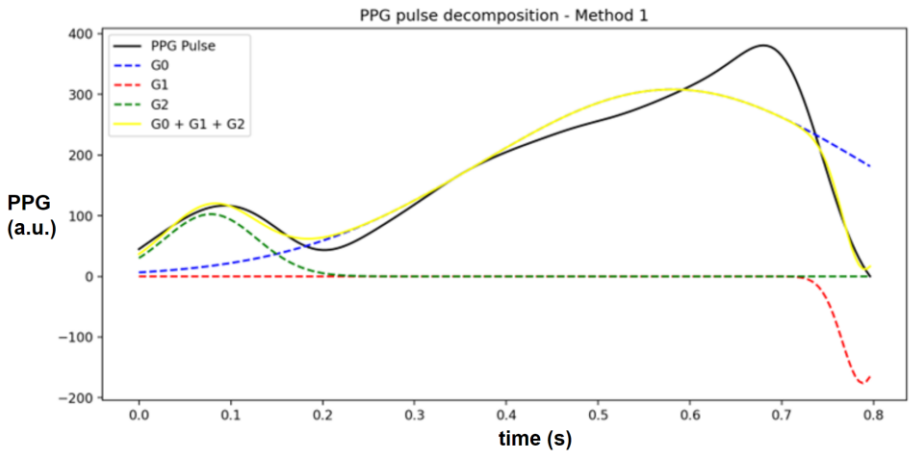

Figure 4.20: Decomposition of the whole CardioHolter pulse in a sum of 3 Gaussians.

The goodness-of-fit for the modelled pulse is for the CardioHolter: $MA_{\%}$ = 88.30% and $RMS_{\%}$ = 81.56%

The Gaussian characteristics A, σ and m are compared in Table 4.2. According to those results, the decomposition is therefore very different for the Empatica pulse and for the CardioHolter pulse.

Table 4.2: Pulse decomposition characteristics for the Empatica and CardioHolter pulses with the 1st decomposition method.

	Empatica			**CardioHolter**		
	G0	**G1**	**G2**	**G0**	**G1**	**G2**
A	0.026	0.008	-0.003	307.8	-175.9	102.5
σ	0.24	0.04	0.05	0.21	0.02	0.05
m	0.49	0.14	0.32	0.58	0.79	0.08

In the second case (Empatica: Figure 4.21, CardioHolter: Figure 4.22), the right pulse is decomposed in a sum of 2 Gaussians ($G0_{right}$ and $G1_{right}$) and then the left pulse is decomposed in a sum of 2 other Gaussians ($G0_{left}$ and $G1_{left}$).

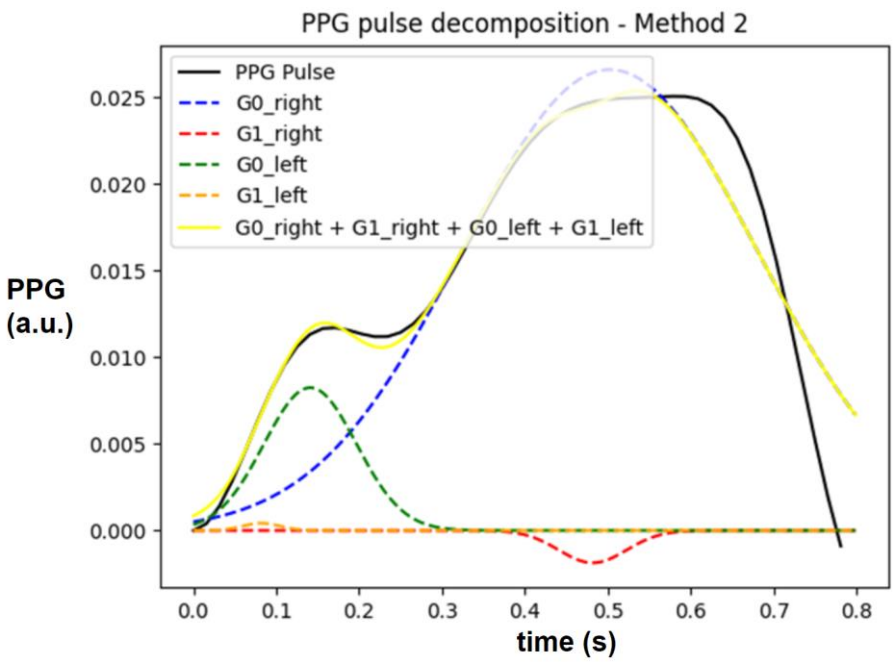

Figure 4.21: Decomposition of the 2 peaks of the Empatica pulse in 2 Gaussians each.

The correlation analysis is for the Empatica pulse:

$MA_{\%}$ = 92.20% and $RMS_{\%}$ = 85.58%

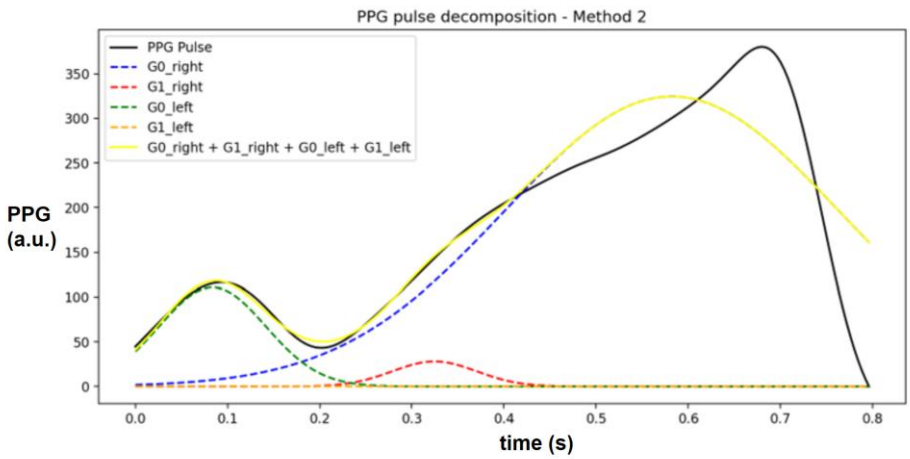

Figure 4.22: Decomposition of the 2 peaks of the CardioHolter pulse in 2 Gaussians each.

The correlation analysis is for the CardioHolter pulse:

$MA_{\%}$ = 86.54% and $RMS_{\%}$ = 76.55%

As for the 1st decomposition method, the decomposition is very different for the Empatica pulse and for the CardioHolter pulse according to the pulse decomposition coefficients (Table 4.3).

Table 4.3: Pulse decomposition characteristics for the Empatica and CardioHolter pulses with the 2nd decomposition method.

	Empatica				**CardioHolter**			
	G0_right	**G1_right**	**G0_left**	**G1_left**	**G0_right**	**G1_right**	**G0_left**	**G1_left**
A	0.027	-0.002	0.08	0.001	324.7	28.0	110.9	0.0004
σ	0.20	0.04	0.06	0.01	0.18	0.05	0.06	0.02
m	0.50	0.48	0.14	0.08	0.58	0.32	0.084	0.082

Due to different PPG signal waveform, the decomposition of the pulse in a sum of Gaussians by both ways is different for the CardioHolter and for the Empatica. However, it can still be used as it the decomposition in Gaussians fits the pulse as efficiently as for the CardioHolter.

Discussion

Critical review of the results

Results from this study demonstrates that a potential replacement of the CardioHolter by the combination of the Empatica and the Faros devices is possible for some specific studies. It is convincing that the analyze of the heart rate, the heart rate variability and the PPG pulse decomposition show a signal quality at least as good for the Empatica and Faros devices as the CardioHolter.

Surely, the impossibility to synchronize the Empatica and the Faros clocks is disappointing, as is the pulse transit time computation, but it is exposed in this thesis that the pulse transit time is not the only interesting characteristic of the PPG and ECG signals. Indeed, many studies on the heart pulses behaviors are based on the heart rate ([27], [31], etc.), the heart rate variability ([10], [15], [16], etc.) and the PPG pulse decomposition ([8], [17], [22], [32], [7], etc.).

Moreover, the CardioHolter is not comfortable and deprives the user of a part of its mobility whereas the Empatica device is a simple wristband, and the Faros device is way less bulky than the CardioHolter. The wearability is so much convenient with the Faros and the Empatica devices that those devices will open the door to new studies, which were impossible with the CardioHolter.

Study limitations

The first limitation of this thesis is the diversity of participants. Indeed, measurements have been made on only one participant. Every person has a different pulse shape, a different heart rate and heart rate variability so it could have been interesting to compare results from several participants. As the focus was on the quality of the devices and the signal processing was time-consuming, it has been decided not to multiply measurements and focus on the signal's quality for one participant.

For the same reasons, it would also have been coherent to proceed measurements in various conditions. It would have been specially interesting on a participant while riding an exercise bike as a future study will be led by the department on biking participants. However, it has never happened for the same reasons as for the participants diversity and the inability to have access to a training bike.

The last limitation for this thesis is the lack of robustness of the PPG pulse decomposition algorithm. It has been decided to decompose a representative PPG pulse acquired with the Empatica wristband device and its corresponding pulse acquired with the CardioHolter because the algorithm does not decompose all the pulses of a signal as it is expected.

Those three limitations made the study based on one specific measurement, but it would have been better to compare various measurements and display them on Bland-Altman plots [33].

Ethics

There is not any ethical concern for this thesis. Indeed, the equipment is safe and has previously been approved for use in clinical studies. Furthermore, I was the only participant of this study.

Future work

Following this thesis, future works can be led. Of course, if a way to synchronize the Empatica and Faros clocks is found, then the combination of those devices would definitively replace the CardioHolter. But even without it, as those devices as comfortable to wear and easy to use, it is now possible to lead studies needing participants to wear the devices for a long term or in motion (for example participants having a physical activity while wearing the devices) while the pulse transit time is not studied.

Conclusion

The aim of this thesis was to study the possibility of replacing the CardioHolter by the combination of the Empatica Embrace + and the eMotion Faros 360. Three main characteristics have been studied from the PPG and ECG signals acquisition: the heart rate, the pulse transit time and the PPG pulse decomposition.

For the heart rate, the results are very similar for all devices, whether it is for the quality of the peak detection, the heart rate computation or the heart rate variability computation. For the Empatica, the pulse decomposition is different from the CardioHolter one but as computable.
However, the impossibility of synchronizing the Empatica and the Faros devices and the inconsistency of the lag between both signals make it impossible to compute a faithful and reliable pulse transit time.

In conclusion, both the Faros and the Empatica signals have an excellent quality and could replace the CardioHolter individually for studies where PTT is not needed but the CardioHolter remains the device to use for PTT computation.

References

[1] F. Nebeker
Golden accomplishments in biomedical engineering.
*IEEE Engineering in Medicine and Biology Magazine (*21), 2002.

[2] Kyeonghye Guk, Gaon Han, Jaewoo Lim, Keunwon Jeong, Taejoon Kang, Eun-Kyung Lim and Juyeon Jung
Evolution of Wearable Devices with Real-Time Disease Monitoring for Personalized Healthcare.
*Nanomaterials (*9), 2019.

[3] Filippo Castiglione, Vanessa Diaz, Andrea Gaggioli, Pietro Liò, Claudia Mazzà, Emanuela Merelli, Carel G. M. Meskers, Francesco Pappalardo and Rainer Von Ammon
Physio-Environmental Sensing and Live Modeling.
*Interactive Journal of Medical Research (*2), 2013.

[4] Sergej Sosunkevic, Andrius Rapalis, Mindaugas Marozas, Vilma Plusciauskaite, Lina Surgaute and Arunas Lukosevicius
Assessment of Multimodal Reactions on Specific Stimulation Tests for Revealing Early Risk of Diabetic Foot.
IEEE, 2018.

[5] Christian Müller, Ulf Hengstmann, Michael Fuchs, Martin Kirchner, Frank Kleinjung, Harald Mathis, Stephan Martin, Ingo Bläse and Stefan Perings
Distinguishing atrial fibrillation from sinus rhythm using commercial pulse detection systems: The non-interventional BAYathlon study.
*Digital Health (*7), 2021.

[6] Tendai Rukasha, Sandra I. Woolley and Tim Collins
Wearable epilepsy seizure monitor user interface evaluation.
ACM, 2020.

[7] Andrew Dykyy, Yuriy Vountesmery, Sergey Mamilov and Illya Chaikovsky
Photoplethysmographic Waveforms Analysis and Classification.
IEEE, 2022.

[8] Navid Hasanzadeh, Mohammad Mahdi Ahmadi and Hoda Mohammadzade
Blood Pressure Estimation Using Photoplethysmogram Signal and Its Morphological Features.
*IEEE Sensors Journal (*20), 2020.

[9] Seungmin Lee, Hyunsoon Shin and Chanyoung Hahm
Effective PPG sensor placement for reflected red and green light, and infrared wristband-type photoplethysmography.
IEEE, 2016.

[10] Mimma Nardelli, Nicola Vanello, Guenda Galperti, Alberto Greco and Enzo Pasquale Scilingo
Assessing the Quality of Heart Rate Variability Estimated from Wrist and Finger PPG: A Novel Approach Based on Cross-Mapping Method.
*Sensors (*20), 2020.

[11] Pablo Armañac-Julián, Spyridon Kontaxis, Andrius Rapalis, Vaidotas Marozas, Pablo Laguna, Raquel Bailón, Eduardo Gil and Jesús Lázaro
Reliability of pulse photoplethysmography sensors: Coverage using different setups and body locations.
Frontiers in electronics, 2022.

[12] Giulia Regalia, Francesco Onorati, Matteo Lai, Chiara Caborni and Rosalind W. Picard
Multimodal wrist-worn devices for seizure detection and advancing research: Focus on the Empatica wristbands.
*Epilepsy Research (*153), 2019.

[13] Suyi Li, Lijia Liu, Jiang Wu, Bingyi Tang and Dongsheng Li
Comparison and Noise Suppression of the Transmitted and Reflected Photoplethysmography Signals.
BioMed Research International, 2018.

[14] Tanveer Syeda-Mahmood, David Beymer and Fei Wang
Shape-based Matching of ECG Recordings.
IEEE, 2007.

[15] Brian W. Johnston, Richard Barrett-Jolley, Anton Krige and Ingeborg D. Welters
Heart rate variability: Measurement and emerging use in critical care medicine.
Journal of the Intensive Care Society, 2020.

[16] Fred Sahher and J.P. Ginsberg
An Overview of Heart Rate Variability Metrics and Norms.
*Front Public Health (*5: 258), 2017.

[17] T. W. B. John J. Sollers
Comparison of the ratio of the standard deviation of the R–R interval and the root mean squared successive differences (SD/rMSSD) to the low frequency-to-high frequency (LF/HF) ratio in a patient population and normal healty controls.
Biomedical Sciences Instrumentation, 2007.

[18] S. N. Kounalakis and N. D. Geladas
The Role of Pulse Transit Time as an Index of Arterial Stiffness During Exercise.
*Cardiovascular Engineering (*9), 2009.

[19] Youna Marc-Derrien, Louise Gren, Katrin Dierschke, Maria Albin, Anders Gudmundsson, Aneta Wierzbicka and Frida Sandberg
Acute Cardiovascular Effects of Hydrotreated Vegetable Oil Exhaust.
Frontiers in Physiology, 2022.

[20] Alan Mathewson, Brian Mark Mccarthy and Brendan O'Flynn
An Investigation of Pulse Transit Time as a Non-Invasive Blood Pressure Measurement Method.
Journal of Physics Conference Series, 2011.

[21] Teng Xiao-Fei and Zhang Yuan-Ting
Theoretical Study on the Effect of Sensor Contact Force on Pulse Transit Time.
*IEEE Transactions on Biomedical Engineering (*54), 2007.

[22] Uldis Rubins
Finger and ear photoplethysmogram waveform analysis by fitting with Gaussians.
*Medical & Biological Engineering & Computing (*46), 2008.

[23] Y. Meyer
Wavelets and Operators.
Cambridge University Press, 1993.

[24] Aneta Wierzbicka, Annette Krais, Frida Sandberg, Katrin Dierschke, Jörn Nielsen, Joakim Pagels, Louise Gren, Monica Kåredal and Anders Gudmundsson
Health effects on humans of emissions from vehicles operated with biodiesel, 2020.

[25] Jiapu Pan and Willis J. Tompkins
A Real-Time QRS Detection Algorithm.
*IEEE Transactions on Biomedical Engineering (*BME-32), 1985.

[26] R. P. Smith, J. Argod, J. L. Pepin and P. A. Levy
Pulse transit time: an appraisal of potential clinical applications.
*Thorax (*54), 1999.

[27] Gerald S. Zavorsky
Evidence and Possible Mechanisms of Altered Maximum Heart Rate With Endurance Training and Tapering.
*Sports Medicine (*29), 2000.

[28] Y. Marc-Derrien
Cardiovascular effects of exposure
to biodiesel exhaust.
Lund University, 2021.

[29] A. V. Kovalenko, S. M. Vovk and Ye G. Plakhtii
Sum Decomposition Method for Gaussian Functions Comprising an Experimental Photoluminescence Spectrum.
*Journal of Applied Spectroscopy (*88), 2021.

[30] T. Chai and R. R. Draxler
Root mean square error (RMSE) or mean absolute error (MAE)?
*Geoscientific Model Development Discussions (*7), 2014.

[31] G. O. Aleksander Perski, Christian Landou, Ulf de Faire, Töres Theorell, Anders Hamsten
Minimum heart rate and coronary atherosclerosis: Independent relations to global severity and rate of progression of angiographic lesions in men with myocardial infarction at a young age.
American Heart Journal, 1992.

[32] Spyridon Kontaxis, Eduardo Gil, Vaidotas Marozas, Jesus Lazaro, Esther Garcia, Mar Posadas-De Miguel, Sara Siddi, Maria Luisa Bernal, Jordi Aguilo, Josep Maria Haro, Concepcion De La Camara, Pablo Laguna and Raquel Bailon
Photoplethysmographic Waveform Analysis for Autonomic Reactivity Assessment in Depression.
*IEEE Transactions on Biomedical Engineering (*68), 2021.

[33] Davide Giavarina
Understanding Bland Altman analysis.
*Biochemia Medica (*25), 2015.